

This is an Open Access document downloaded from ORCA, Cardiff University's institutional repository:<https://orca.cardiff.ac.uk/id/eprint/153069/>

This is the author's version of a work that was submitted to / accepted for publication.

Citation for final published version:

Ling, Jiaxin, Li, Xiaojun, Li, Haijiang , Shen, Yi, Rui, Yi and Zhu, Hehua 2022. Data acquisition-interpretation-aggregation for dynamic design of rock tunnel support. Automation in Construction 143 , 104577. 10.1016/j.autcon.2022.104577

Publishers page: <http://dx.doi.org/10.1016/j.autcon.2022.104577>

Please note:

Changes made as a result of publishing processes such as copy-editing, formatting and page numbers may not be reflected in this version. For the definitive version of this publication, please refer to the published source. You are advised to consult the publisher's version if you wish to cite this paper.

This version is being made available in accordance with publisher policies. See <http://orca.cf.ac.uk/policies.html> for usage policies. Copyright and moral rights for publications made available in ORCA are retained by the copyright holders.



Data acquisition-interpretation-aggregation for dynamic design of rock tunnel support

Jiaxin Ling ^a, Xiaojun Li ^{a,*}, Haijiang Li ^{b,*}, Yi Shen ^a, Yi Rui ^a, Hehua Zhu ^a

a Department of Geotechnical Engineering, Tongji University, 1239 Siping Road, Shanghai 200092, China

b School of Engineering, Cardiff University, UK

Abstract: During the rock tunnel construction, one of the critical aspects lies on the support design to secure the construction safety. Due to the extreme complex underground geological and geotechnical condition, the support design needs to be dynamic and ideally should consider all related data and information comprehensively and timely. Different Internet of things (IoT) and other related information technologies (IT) have been widely applied during tunnel construction to collect a large amount of monitoring data, which in turn demands real time or just-in-time (JIT) data processing for decision making. To understand the state-of-the-art IoT-based dynamic tunnel support design, a comprehensive review is conducted from the perspectives of real time or just-in-time data acquisition, data interpretation and data aggregation. For different types of technologies, their time consumptions, technology strengths and drawbacks were thoroughly analyzed in a full and seamless “data acquisition-interpretation-aggregation” workflow linking to the dynamic tunnel support optimum design. As a result of the review, three primary research gaps are identified, i.e., the high time consumption of data interpretation, dilemmas of conventional and AI-supported aggregation methods, and long retrieval time for similar design cases. Focusing on these three gaps, three key concepts, namely, time consumption, accuracy, and degree of automation, are proposed as key indicators for the tunnel support design. A conceptual framework, just-in-time tunnel support design is further proposed, where the most appropriate and efficient methods can be conceptually integrated and lead towards technical implementation. This review contributes to the comprehensive understanding of timely dynamic tunnel support design and provides future insights of promoting JIT

29 tunnel support optimum design.

30 **Key words:** rock tunnel, tunnel support design, just-in-time, Internet of things,
31 information technology, drill and blast method

32 **1 Introduction**

33 The drill and blast (D&B) method is a typical and conventional method for the
34 excavation of tunnels in rocks as it enables the flexibility to excavate varying tunnel
35 cross-sections and possibility of adapting to changing rock mass conditions [1,2]. The
36 design of tunnels constructed using the D&B method involves many aspects, including
37 the determination of the geometric layout, and shape and size of the profile; nonetheless,
38 the design of the support used on site is a key issue[3].

39 Tunneling, as a typical geotechnical engineering, is characterized by a high level
40 of uncertainty, posing a unique challenge to design work compared to other civil
41 engineering projects [4,5]. As the comprehensive interpretation of the geological and
42 geotechnical characteristics of the underground environment is difficult, the design of
43 rock tunnel support is generally composed of preliminary and final design stages [6].
44 In the preliminary design stage, engineers determine support systems and parameters
45 based on the sparse data collected from geological investigations (e.g., the ground
46 surface survey, borehole investigation). However, owing to the sparsity of the data,
47 inherently, the design scheme of the support may fail when unanticipated geological
48 conditions are encountered during tunneling, which is proved by many accidents arising
49 from incomplete geological knowledge [7]. Hence, engineers must optimize the support
50 parameters according to the data exposed by excavation to complete the final design of
51 the support. In particular, the optimization of the support parameters depends on the
52 geology of the tunnel face, deformation of the surrounding rock and stress-strain in
53 support structures [8]. The design method, which implements the final design of the
54 support by revising the preliminary design using the exposed geological conditions and
55 various unanticipated conditions during the construction process, is also called the
56 dynamic design of the support [6,9]. It is worth mentioning that the concept of the

57 dynamic design of the tunnel support has been suggested by several national standards
58 and specifications [10,11].

59 The dynamic design of the support of the tunnel excavated by the D&B method
60 faces one critical technical challenges: the quick response of the support, which stems
61 from the fact that untimely support under poor geological conditions may pose a
62 significantly higher risk to the tunnel stability [12]. Hence, the acquisition of the data
63 exposed by excavation, interpretation, and aggregation of the data during the tunnel
64 construction should be fast. Here, the term “aggregation” instead of the term “analysis”
65 is used because the processing of the interpreted data in tunnel engineering includes
66 both the conventional analyses, such as the numerical analysis, and informatics-related
67 methods. Indeed, the term “aggregation” incorporates the meaning of conventional
68 analysis and new-emerging informatics-based processing. The prerequisite for an
69 optimal determination of the support parameters in the construction process is an
70 appropriate estimate of the exposed data as well as the mechanical response [5].
71 Therefore, firstly, an efficient on-site data acquisition method can significantly
72 contribute to the dynamic design of the tunnel support. Conventionally, the data on or
73 ahead the tunnel face are sketched by field engineers using hand-held equipment, such
74 as a geological compass, measuring tape and roughness profile gauge [13], which is
75 time-consuming and error-prone. With the advancement of IoT in recent years,
76 techniques such as digital photogrammetry (DP) [13,14] and terrestrial laser scanning
77 (TLS) [15,16] have been introduced into the tunnel support design because of their great
78 potential to shorten the data acquisition time and improve the data acquisition accuracy.
79 In addition, many practical engineering cases have demonstrated the advantages of IoT
80 in assisting the efficient acquisition of exposed data on site [16,17]. Based on the
81 acquired raw data, several efficient interpretation methods have been proposed to obtain
82 the required information, such as discontinuity and water inflow information, which
83 can reduce errors in manual interpretations. Another key concern affecting the dynamic
84 design of the support is the aggregation of interpreted data. Conventional aggregation

85 methods include empirical, numerical and analytical analysis, the combination of which
86 has also been adopted in some complex cases, where numerical and analytical methods
87 are used to verify the parameters provided by empirical methods [6]. However, the
88 selection of proper mathematical parameters and sensitivity to the mesh and boundary
89 effects may cost the numerical and analytical models a long period of time to yield [18].
90 Hence, aggregation methods, such as simplified analytical models [18] and the
91 parallelization of numerical models [19], which are more intuitive and computationally
92 efficient, are gradually developed to assist the design of the tunnel support,. In addition,
93 several artificial intelligence (AI)-based computational methods, such as genetic
94 algorithm (GA) and artificial neural network (ANN), have been used to complement
95 the results from construction sites to optimize the support design in a short period of
96 time, because AI offers predictive capabilities to improve the efficiency and reliability
97 of the design process [20]. Moreover, the advancements in IoT and IT have
98 demonstrated conceivable benefits in the dynamic design of the tunnel support. The
99 focuses on the capabilities of data acquisition, data interpretation and data aggregation
100 have reached an unprecedented level owing to their increasing dependence on IoT and
101 IT. Indeed, IoT-based acquisition approaches integrated with IT-driven interpretation
102 and aggregation solutions provide a new direction for the dynamic design of the tunnel
103 support.

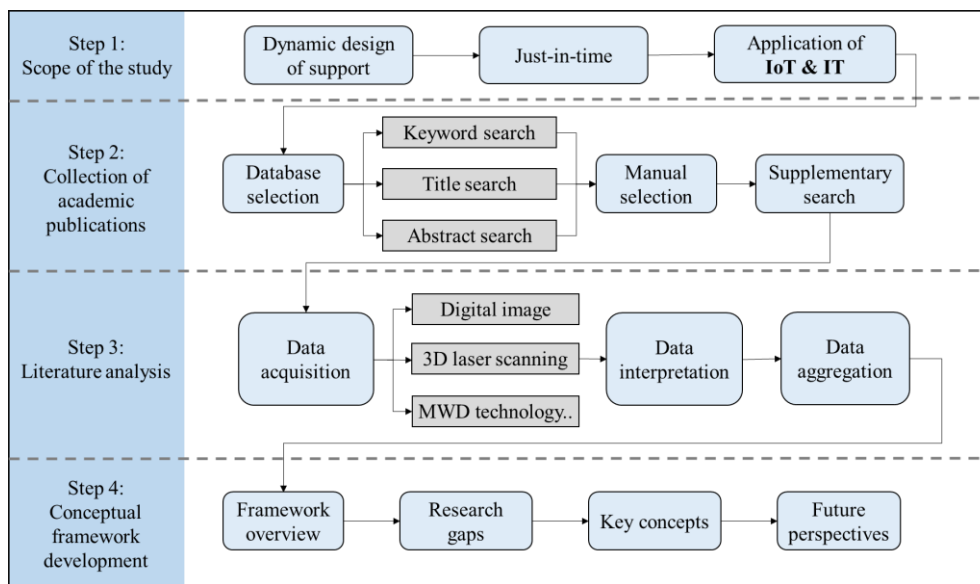
104 Due to the popularity of applying dynamic design in the construction process of
105 tunnels using the D&B method, several review articles have summarized the state-of-
106 the-art advancements in the rock mass blastability [21], automatic extraction of
107 discontinuity parameters [22] and tunnel ahead prospecting [23]. Although these
108 reviews have summarized some aspects of the dynamic design and information-based
109 tunnel construction, certain limitations exist that (1) none of the existing studies
110 thoroughly summarize the comprehensive aspects of the dynamic design of the tunnel
111 support from data acquisition to data interpretation and aggregation. In addition, the use
112 of IoT in the dynamic design of the tunnel support has brought a paradigm shift to rock

113 engineering design [6]. However, none of the existing reviews were conducted from the
 114 perspective of IoT-based dynamic design of the tunnel support; (2) key research
 115 directions of the techniques and their applications in the design of the tunnel support
 116 have not been discussed. To address these knowledge gaps, this study aims to provide
 117 a thorough review of IoT-based dynamic design of the tunnel support, with a focus on
 118 the quick acquisition of data during construction, interpretation of the raw data, and
 119 aggregation of the interpreted data. In addition, research gaps are discussed, and the
 120 conceptual framework of the JIT design of rock tunnel support is proposed.

121 2 Research methodology

122 This study provides an in-depth overview and analysis of the recent advances in
 123 IoT-based dynamic design of the tunnel support. To address the existing knowledge
 124 gaps, the research approach of the study is divided into four steps, as presented in

125 **Fig.1:**



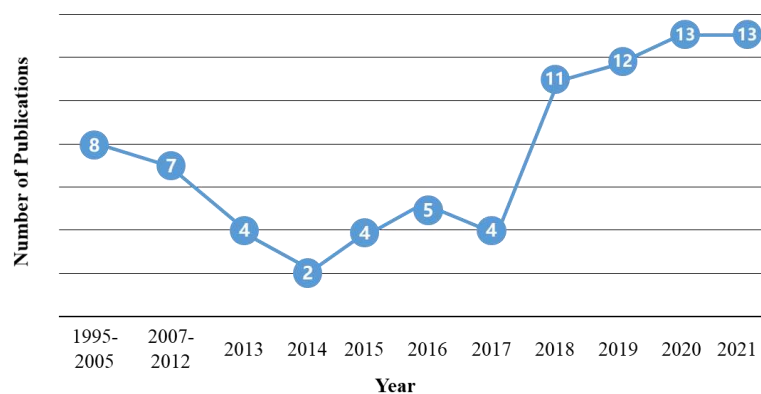
126

127 Fig.1 Flow chart of research methodology

128 1) Clarify the scope of the study: The IoT-based dynamic design of the support in
 129 rock tunnels constructed by the D&B method was the primary research aim; therefore,
 130 literatures regarding tunnels constructed by a tunnel boring machine (TBM) were not
 131 considered. Moreover, the emphasis of the study focused on the optimization of the
 132 support parameters using on-site data, so studies that employed data from the

133 preliminary stage to determine support schemes were not reviewed.

134 2) Collect academic publications: Studies on the fast acquisition, interpretation,
135 and aggregation of on-site data during tunneling were thoroughly reviewed. Two
136 comprehensive and representative academic databases, Scopus and Web of Science
137 (WoS), were adopted as sources of literature. The first screening of the literature
138 retrieval started with searching keywords and key strings including “tunnel support
139 design”, “information technology”, “Internet of thing”, “artificial intelligence”,
140 “dynamic design” and “tunnel face information”. Subsequently, the search results
141 were analyzed using the title, keywords, and abstract to retain the most appropriate
142 literature within the scope of this study. Moreover, some additional keywords, such as
143 “photogrammetry” and “measurement while drilling (MWD)”, were identified. Hence,
144 a second screening using the new keywords and key strings was performed as a
145 supplementary search. The results of the second search were manually filtered to
146 identify appropriate studies; 83 publications were identified. **Fig.2** shows the yearly
147 distribution of the 83 bibliographic records in the Scopus and WoS databases. Before
148 2017, few studies were conducted on the quick acquisition, interpretation, and
149 aggregation of data during the tunnel construction. However, the peak points occurred
150 after 2018. With the advancement of IoT, more studies were conducted on the quick
151 acquisition, interpretation, and aggregation of data concerning the dynamic design of
152 the tunnel support.

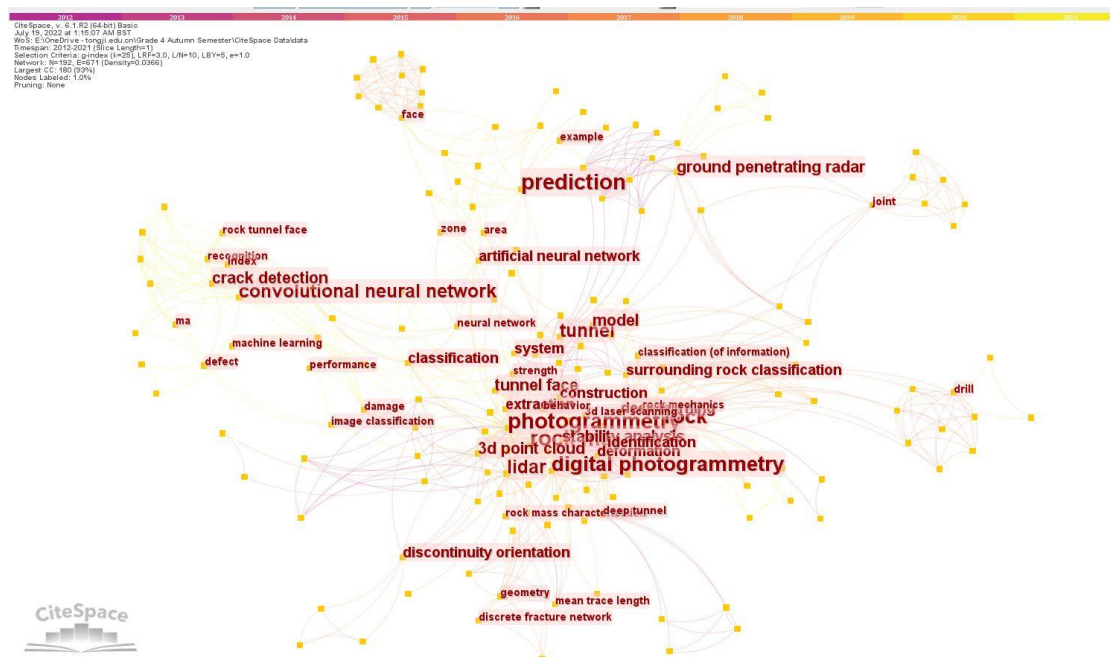


153

154 Fig.2 Year and number of reviewed articles on design of tunnel support.

155 Additionally, we used CiteSpace, a Java application for analyzing and visualizing

156 co-citation networks, to conduct a scientometric analysis [24]. A network of co-
 157 occurring keywords was generated using CiteSpace containing 192 nodes and 671
 158 links, as shown in **Fig.3**. In this network, the label size was determined by the
 159 frequency of the keyword in the bibliometric record. The top 10 frequently-used
 160 keywords are “photogrammetry”, “rock mass”, “prediction”, “light detection and
 161 ranging (LiDAR)”, “convolutional neural network”, “3D point cloud”, “stability
 162 analysis”, “tunnel face”, “ground penetrating radar” and “crack detection”. It can be
 163 seen that keywords, such as the photogrammetry, LiDAR, and ground penetrating
 164 radar, that were associated with the fast data acquisition methods appeared most
 165 frequently, followed by data aggregation methods, such as the convolutional neural
 166 network and stability analysis. Furthermore, the results verified that the literature was
 167 dominantly reviewed from the data acquisition, interpretation, and aggregation point
 168 of view.



169

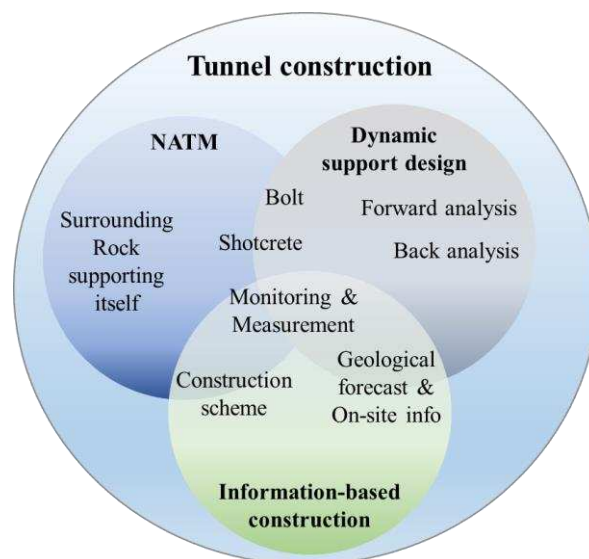
170 Fig.3 Network of co-occurring keywords in the reviewed papers

171 3) Conduct the literature analysis: The reviewed studies were analyzed concerning
 172 the theme of IoT-based dynamic design of the tunnel support. The analysis included
 173 the quick acquisition of on-site data using different IoT-enabled equipment,
 174 interpretation of the acquired data, and optimization of the support parameters using

175 efficient computational aggregation methods.

176 4) Develop the conceptual framework: First, the framework was defined and
177 overviewed; subsequently, the research gaps of the existing studies were identified.
178 Accordingly, the key concepts influencing the design of the tunnel support were
179 summarized. Finally, a conceptual framework was developed to completely elucidate
180 the steps required for the JIT design of the tunnel support. Additionally, future
181 perspectives of the proposed JIT design of the tunnel support were discussed.

182 The dynamic design of the support is usually associated with the “information-
183 based construction” and “new Austrian tunneling method (NATM)” terms. Therefore,
184 the relationships and differences between these terms need to be clarified to
185 profoundly comprehend the meaning of the dynamic design of the tunnel support. The
186 relationships between dynamic design of tunnel support, NATM and information-
187 based construction are presented in **Fig.4**.



188
189 Fig.4 Relationships and differences between the dynamic design of the tunnel support,
190 NATM and information-based construction

191 NATM was first proposed in 1964 [25] and its fundamental principle is to
192 maximize the capacity of surrounding rock to sustain its own weight in the
193 construction process. After several years of development, NATM has incorporated
194 many existing excavation and support methods. However, one of its core parts is
195 timely monitoring and measurement of the surrounding rock and structure [8].

196 Moreover, shotcrete, bolts, and monitoring are considered to be the key elements of
197 NATM in the construction of rock tunnels.

198 Information-based construction refers to the application of IT in tunnel
199 construction to collect, store and process on-site data to provide a decision-making
200 basis for the design and construction processes [26]. Similar to NATM, information-
201 based construction also includes monitoring and measurement using different
202 intelligent sensors. Moreover, advanced geological forecast and on-site data
203 acquisition using different intelligent measuring equipment are within the scope of the
204 information-based construction.

205 As mentioned above, the dynamic design of the support is a process, in which the
206 preliminary design is optimized based on the data exposed during construction. It
207 relies on the ahead geological prospecting, measurement of tunnel face data, and
208 monitoring data, which are the outcome of information-based construction and NATM.
209 Accordingly, forward and back analysis can be conducted using these data. Moreover,
210 the quick dynamic design of tunnel supports primarily depends on the tunnel face and
211 ahead geological prospecting data, because the monitoring data might need a long
212 duration [27]. In this study, we investigated the quick acquisition of tunnel face and
213 advanced geological data of NATM or information-based construction; in addition,
214 we considered the corresponding efficient interpretation and aggregation methods to
215 provide a profound comprehension of the dynamic design of the tunnel support.

216 **3 Quick acquisition of data during construction**

217 Two types of data acquisition methods have been used to obtain on-site data
218 quickly: noncontact measuring techniques to record tunnel face data, and ahead
219 geological prospecting techniques to reflect geological/hydrogeological conditions in
220 front of the tunnel face. The application of IoT in the quick acquisition of data during
221 the construction process of a rock tunnel from these two aspects are discussed.

222 **3.1 Digital photogrammetry**

223 The recording of on-site tunnel face data typically involves handheld tools, such

224 as measuring tapes and geological compass-clinometers, which need to be operated
225 manually [13]. In most cases, this tedious process is labor-intensive, error-prone and
226 more importantly, time-consuming [28]. Due to the simplicity of obtaining data and the
227 possibility of interpreting data accurately, DP has been employed in rock engineering
228 since the 1970s [29]; in addition, it has been used in tunnel sites in many countries, such
229 as Italy [30], China [17,31], Spain [32]. This approach has been satisfactorily adapted
230 to tunneling activities because uncertain geological conditions require regular and
231 frequent updates to geological surveys. Accordingly, photogrammetry techniques, such
232 as the structure-from-motion technique, and aggregation algorithms have been
233 gradually developed to enable faster and more accurate data acquisition.

234 In the tunnels constructed using the D&B method, after blasting and mucking, a
235 digital camera is typically placed to the tunnel face to be mapped. Generally, the camera
236 is placed in front of the tunnel face, and images of the tunnel face are recorded from a
237 certain point of view, as shown in **Fig.5** (a). Monocular image systems have been widely
238 adopted in earlier studies, and many image processing algorithms have been introduced
239 to extract the required data accordingly. Due to the simplicity of DP, each image of the
240 tunnel face usually needs less than 1 min to be captured [33]. However, monocular
241 image systems can only record 2-dimensional (2D) data, failing to record relevant 3-
242 dimensional (3D) data of the exposed rock mass. Hence, binocular image system and
243 structure from motion technology, which can acquire 3D data using multiple images
244 from different views [32,34], as shown in **Fig.5** (b) and (c), have been gradually and
245 widely used in the acquisition of the tunnel face data. The entire process, from the
246 preparation to camera displacements and capturing pictures, usually takes
247 approximately 10 ~ 30 min [32,35,36]. Huang et al. [28] demonstrated that the time
248 required to acquire the tunnel face data using DP was approximately 1 h because
249 additional procedures, such as the arrangement of control points and use of a total
250 station to survey the control points, were included. By comparison, the conventional
251 manual sketch of the exposed tunnel face data can take as long as 4 h to acquire the data

252 due to the dark and narrow environment of the underground tunnel [28]. Thus, the
253 application of DP in acquiring the tunnel face data during construction can significantly
254 improve the efficiency of data acquisition.

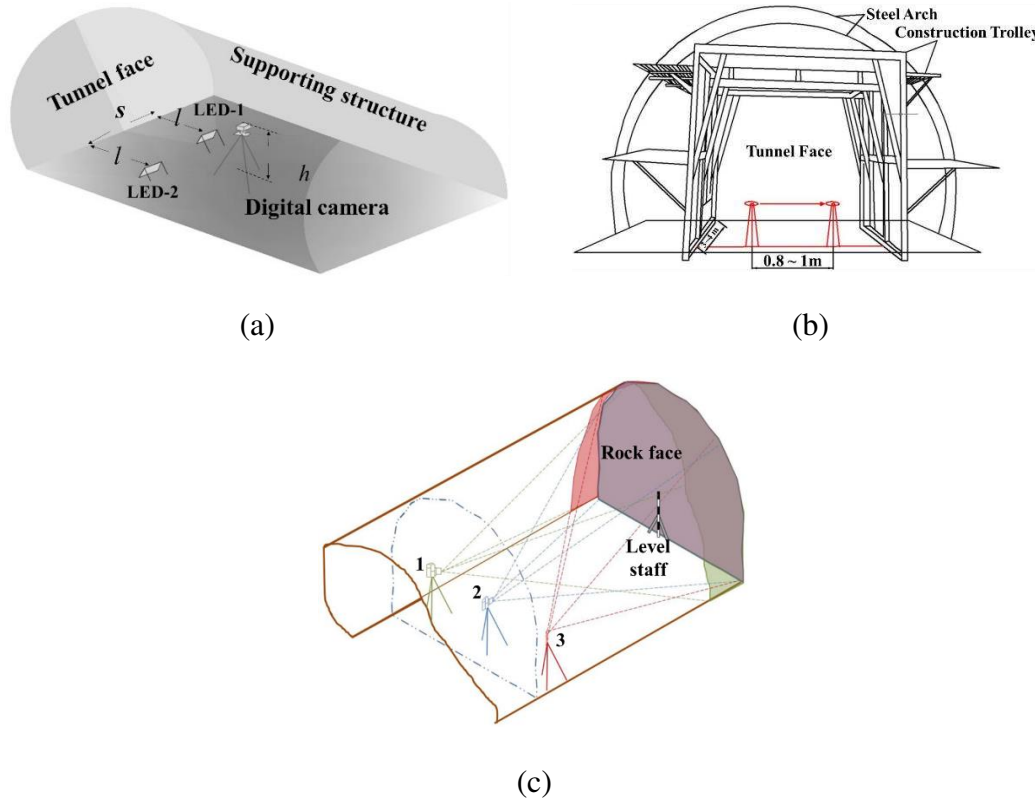


Fig.5 Different layouts of digital cameras: (a) Monocular image system [17]. (b) Binocular image system [37]. (c) Structure from motion technique [30]

255 3.2 Terrestrial laser scanning

256 With the advancements in LiDAR, TLS technology has proven to be a useful and
257 efficient noncontact tool for the acquisition of rock mass data, which functions using
258 the controlled steering of a laser beam coupled to a high-speed motorized system that
259 incrementally scans a specific field of view using a rotating mirror [38-40]. In principle,
260 laser pulses transmitted by scanners are reflected off physical objects; thus, they
261 generate a large number of 3D data points (point cloud data) that record the position (x ,
262 y , z) in the space and reflectivity (i) of the physical objects [41]. Processing and
263 aggregation can be conducted using the generated point cloud data to extract the
264 required information. Compared with DP, TLS is less prone to occlusions, and its
265 measurement accuracy is not affected by lighting conditions [42]. Hence, whilst TLS

266 has far found limited use in the rock tunnel due to the specialist equipment required,
267 the fact that the measurement accuracy can be guaranteed makes it a promising
268 technique for application in rock tunnel construction. Indeed, TLS has been applied in
269 many tunnel construction sites, such as Yuexi [43], Sandvika and Fossvein [16] and
270 Monte Seco [44] tunnels. **Fig.6** depicts the setup of the TLS equipment at a construction
271 site in Norway.



272

273 Fig.6 LiDAR scanning of a tunnel face with a diameter of 10m in Oslo, Norway [41].

274 The time required to scan the tunnel face varies from site to site because the size
275 of the tunnel face to be scanned, distance between the scanner and tunnel face, and
276 resolution of the point cloud can affect the scanning time [45]. Generally, with an
277 acceptable point cloud resolution, the time required to scan a tunnel face can be
278 controlled within 10 min. In [16], the best operational condition was a resolution
279 accuracy of 6 mm, which required 3 min to scan a tunnel face with a diameter of 10 m.
280 Similarly, in [45], the time required to scan a tunnel face with a diameter of 13 m and
281 achieve an appropriate resolution was 5 min and 12 s. In some cases, the scanning time
282 can exceed 30 min to achieve a higher resolution accuracy of 3 mm [39].

283 **3.3 Measurement while drilling technology**

284 In recent decades, the MWD technology has been increasingly used for data
285 acquisition and support optimization during the information-based construction in the
286 D&B tunneling industry. MWD is a technique that captures the responses of drilling
287 parameters on a real time basis, while drilling is underway to expand the knowledge of
288 structural and mechanical properties of the penetrated rock [46-48]. It monitors drilling

289 parameters, such as drilling depth, rotation speed, rotation pressure, penetration rate,
290 percussive pressure, feed pressure, damping/stabilizer pressure, and water/flush
291 pressure [46,47]. Compared with other subsurface exploration methods, such as DP and
292 TLS, MWD (1) offers a lower-cost approach to obtain high-resolution data as both DP
293 and TLS require an expensive camera or scanner to perform the field work; (2) provides
294 a better and more accurate description of the hidden volume of the rock mass because
295 TLS and DP mainly portray the information on the visible portion, which may result in
296 over-estimation of rock mass quality in some cases due to weathering of the tunnel face
297 or poor blasting practices; and, (3) permits faster insight into the structural and
298 mechanical parameters of the rock mass without slowing down the excavation process
299 as data are recorded during the drilling operation [46,49]. Hence, MWD has been
300 increasingly applied to characterize rock masses and provide a basis for the dynamic
301 design of the tunnel support. With these advantages, MWD technologies have been
302 widely used in rock tunnels in many countries, such as Sweden [1,2], Norway [50],
303 Austria [49].

304 The collection of MWD data relies on machinery for tunnel face drilling, that is,
305 jumbo, during the information-based construction. **Fig.7** shows a jumbo at a
306 construction site in Stockholm. As the acquisition of MWD data is completed during
307 the drilling operation, the time spent to collect and analyze data is greatly reduced,
308 which is primarily owing to data processing and aggregation. Generally, data processing
309 involves data importation, noise reduction, parameters extraction and variation
310 detection [49]. Some recent methods consider all effects of the drilling process [47].
311 Hence, the time spent during the entire process should depend on the algorithm used
312 and data size; however, none of the reviewed studies specifically reported the consumed
313 time. Nevertheless, the entire time span of MWD-enabled support design is relatively
314 short, as the processing of MWD data is easier than that of images.



Fig.7 Jumbo at a construction site [47]

315

316

317 **3.4 Other ahead geological prospecting technologies**

318 Ahead geological prospecting is a technique that predicts lithological and

319 structural heterogeneities in front of the tunnel face within a certain range [23]. During

320 tunnel construction, it has become an essential routine that ahead geological

321 prospecting needs to be performed after the exposure of the new tunnel face to obtain

322 the quantitative and qualitative information of the rock mass, which can provide reliable

323 basis for the optimization of the original support schemes [10]. Likewise, this

324 information-based construction approach should also be a quick-response process from

325 data acquisition to data interpretation, as the time interval between the mucking of the

326 previous round and drilling of the next round at the construction site is often

327 considerably short. Therefore, advanced geological prospecting techniques have been

328 developed and increasingly applied in the construction of D&B tunnels. In general,

329 ahead geological prospecting techniques consist of destructive and nondestructive

330 techniques. MWD is one typical example of destructive-ahead prospecting techniques;

331 thus, the destructive-ahead prospecting techniques were not considered in this study. A

332 detailed and comprehensive overview of the application of advanced geological

333 prospecting techniques in tunneling, with an emphasis on the principles, technical

334 levels, trends, and key problems was summarized by Li et al. [23]. Here, different types

335 of ahead geological prospecting technologies and time of acquisition are presented.

336 Based on the detection range, ahead prospecting techniques can be divided into

337 short-distance prospecting (<30m, e.g., ground penetrating radar (GPR)), moderate-

338 distance prospecting (<60m, e.g., transient electromagnetic method (TEM)), and long-
339 distance prospecting (<120m, e.g., tunnel seismic prediction (TSP)) [23]. The time
340 required for each technique to collect on-site data varies slightly. The use of GPR, TSP,
341 and TEM involves the setup of the instrument, layout of the measuring line/blasting
342 points/measuring point, collection of signals, and processing of the acquired data. None
343 of the literature reviewed mentioned a specific time that each technique requires to
344 acquire data. Thus, we interviewed experienced engineers, and realized that GPR and
345 TEM need less than 2 h to collect data depending on the size of the excavation face,
346 length of the measuring line, and number of measuring points, whereas TSP consumes
347 a longer time to acquire data as the explosion holes need to be drilled on the wall.

348 **4 Interpretation of acquired on-site raw data**

349 Raw data, such as images and waves, can be obtained using the acquisition
350 methods, as described in Section 3. Here, different interpretation methods for extracting
351 the required information from the raw data and contribution of the interpreted data to
352 the dynamic design of the tunnel support are discussed.

353 **4.1 Interpretation of DP data**

354 Table 1 summarizes the application of DP in rock tunnel construction.

355 Table 1 Summary of the application of DP in data acquisition

Refs	Information extracted	Approach	Time required	Contribution
[14]	Discontinuity length, orientation, separation width, JRC value	Region growing	NA ^a	Calculation of GSI rating
[51]	Discontinuity trace	feature point based, point cloud data	<2min to extract data	Calculation of RMR or Q value
[13]	Discontinuity trace	ravine-line based	NA	NA
[30]	Orientation of joint sets	Rockscan software	Less than 10min to collect the images	Characterization of rock masses
[52]	Position, shape, spacing of joint set, trace length	Siro 6.0 software	NA	NA
[17]	Fracture length, dip angle, intensity and density of the fracture traces	Deep learning	8h 23min to train model and 0.44s/image for testing	Rock mass classification
[37]	Discontinuity orientation, trace, spacing, roughness, aperture	Improved K-means clustering, point	NA	Calculation of RMR and GSI

		cloud data			
[53]	Joint set, joint spacing, joint angle	Edge detection	NA		Calculation of RQD
[54]	Discontinuity orientation	Improved K-means clustering, point cloud data	about 2.5h to extract data from 382,085 facets		NA
[31]	5 types of rock structures	deep learning	2.163s/image for classification		Automated rock classification
[55]	Discontinuity network emplacement	Edge detection	NA		Identification of block geometry
[56]	Geological features such as joints and cracks	Edge detection	NA		Rock mass rating
[29]	Mean trace length, total trace length, total spacing	Edge and line detection	NA		Calculation of RQD
[57]	Joint and bedding spacing, joint condition	Improved K-means clustering, point cloud data	NA		Calculation of RQD and RMR value
[58]	Weak interlayer	Deep learning	0.633s/image for testing		NA
[34]	The location, dip direction and dip angle of joints	Point cloud data, Halcon software	NA		3D stability analysis
[59]	Shotcrete thickness	Comparison of different images	NA		Mapping shotcrete thickness
[60]	Weak interlayers and fracture traces	Machine learning	300s ~ 700s		Assessing the rock mass quality
[61]	Water inflow	Deep learning, CNN	9.85h to train model and 0.428s/image for testing		Calculation of RMR value
[62]	Length and mean spacing of the trace line	Edge detection	NA		Calculation of Rock Block Index
[63]	Deterministic structural planes, joint orientation data	GeoSMA-3D software	Within 10 minutes		Stability analysis of tunnel blocks
[28]	Dip and dip direction of the discontinuity	CAE Sirovision software	About 1h to acquire data and 1.5h for post-processing		Stability analysis
[32]	Dip and dip direction of discontinuity sets	Discontinuity Set Extractor software	About 30 min to photograph and 22h to process 169 photos		Characterization of rock mass
[35]	Dip and dip direction of the discontinuity	Grouping algorithm, point cloud data	10min to collect data and 15min 34s to operate		Characterization of rock tunnel face
[36]	Dip angle, spacing and length of the joints	Manual sketch	About 20min to collect 68 images		Calculation of RQD
[64]	Rock mass structure categories	Deep learning, CNN	NA		Characterization of rock mass

[65]	Number and spacing of rock joint groups	Deep learning	NA	Calculation of basic quality (BQ) value
[66]	Dip, dip direction, trace length and spacing of joints	Manual sketch	NA	Calculation of RBI value
[33]	Dip, dip direction and trace length of joints	ShapeMetriX3D software	1min to collect data	Stability analysis
[67]	Rock mass fractures	Edge detection	NA	Classification of surrounding rock of the tunnel face

356 ^a NA: not available.

357 Based on the images obtained using DP, several interpretation algorithms have
358 been developed to extract information accurately and timely. Table 1 shows that two
359 different types of processing methods have been used to interpret the images and extract
360 the required information; some methods use raw images and some methods employ the
361 point cloud data. The former focuses on the direct extraction of information from the
362 obtained images while the latter converts images into a 3D point cloud for extraction.
363 As listed in Table 1, raw-image-based methods include the region-growing [14], ravine-
364 line-based [13], and edge detection [29,53,55,56,62,67] methods. Since the principles
365 of these methods are not the focus of this paper, details of the algorithms, such as the
366 pros and cons, are not discussed here (see [22] for details). In addition, with
367 advancements in AI, different AI branches, such as deep learning, have benefited the
368 timely interpretation of the obtained images. Chen et al. extracted fracture trace
369 (fracture length, dip angle, intensity and density of the fracture traces) [17], weak
370 interlayer [58] and water inflow [61] information on the tunnel face from more than
371 3000 raw images using convolutional neural network (CNN) methods. The time to train
372 the model in the three cases was more than 8 h; however, the time required to test the
373 model after a successful train was less than 1 s per image, which was computationally
374 efficient. Moreover, Chen et al. [31] used a CNN-based method to classify the rock
375 structure into five categories using approximately 3,000 raw images captured from 150
376 tunnel faces, where the time to classify a new image after the model training was only
377 about 0.33 s. The latter one, i.e. methods using point cloud data, has also been used by

378 several studies to extract 3D data of the tunnel face for less dependence on the image
379 quality and camera calibration [51]. The images were first converted into point cloud
380 data, and the corresponding aggregation was then conducted based on the point cloud
381 data. Chen et al. [54] used an improved K-means clustering method to extract the
382 discontinuity orientation from tunnel face 3D point clouds; the time consumed to
383 extract information from 382,085 facets was about 2.5 h. To reduce the need for manual
384 intervention and improve computational efficiency, Chen et al. [35] proposed a semi-
385 automatic discontinuity characterization method using 3D point clouds; the operation
386 time was approximately 15 min. Similarly, Zhang et al. [51] extracted the discontinuity
387 trace information using trace feature point; the total processing time was less than 2
388 min. Meanwhile, commercial software and open-source programs, such as Rockscan
389 [30], GeoSMA-3D [63], CAE Sirovision [28] and Discontinuity Set Extractor (DSE)
390 [32], have been gradually developed and applied in the acquisition and interpretation
391 of tunnel face data,. However, the interpretation of images in some software packages
392 may experience a long time as the generation of a high density point cloud is
393 computationally expensive [32].

394 In terms of the information extracted, as presented in Tab.1 and **Fig.8** (a),
395 discontinuity-related (including joint and fracture) studies account for 84% of the
396 reviewed publications, where the length, dip angle, dip direction, spacing, density, and
397 number of discontinuity sets are the main parameters to be extracted. Based on the
398 extracted discontinuity information, two typical subsequent analysis are the
399 characterization and stability analysis of the rock mass. As shown in **Fig.8** (b), the
400 characterization of the rock mass accounts for 2/3 of the subsequent analysis of the
401 extracted information. This analysis usually involves the calculation of the rock quality
402 designation (RQD) value [29,36,53,57], rock mass rating (RMR) value [37,51,57],
403 geological strength index (GSI) value [14,37], and other rock mass rating systems. In
404 addition, RMR has been widely used in many rock tunnel projects as a crucial indicator
405 to define the support parameters [68]. In the RMR system, six basic parameters are used

406 to classify the rock mass; these parameters are the uniaxial compressive strength (UCS)
407 of rocks, RQD value, discontinuity spacing, discontinuity condition, groundwater
408 condition, and discontinuity orientation with respect to the opening axis, while the
409 estimation of RQD is related to the spacing and number of the discontinuities [37]:

$$410 \quad RQD = 115 - 3.3J_v \quad (1)$$

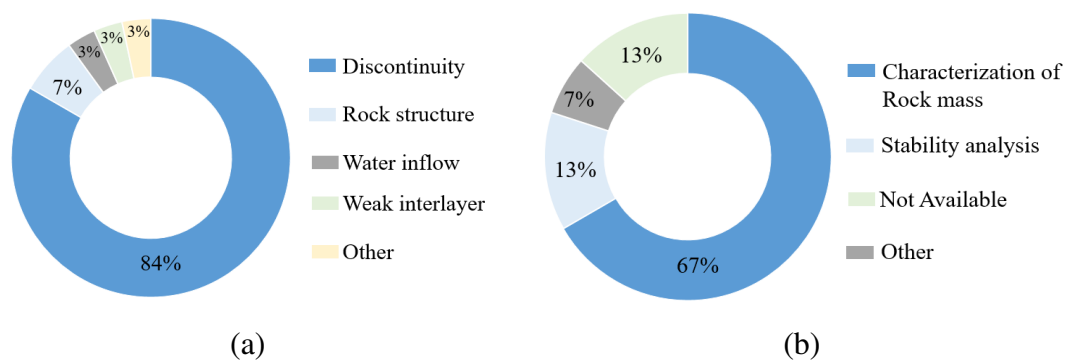
$$411 \quad J_v = \frac{1}{s_1} + \frac{1}{s_2} + \frac{1}{s_3} + \dots + \frac{1}{s_n} + N_r(5\sqrt{S}) \quad (2)$$

412 where s_1, s_2, \dots, s_n denote the mean spacing of each discontinuity set, N_r denotes
413 the number of discontinuities and S is the measuring area.

414 Obviously, the extracted discontinuity information can be applied to calculate the
415 value of RQD or RMR, thereby determining the support parameters. For instance, Lemy
416 et al. [29] extracted the trace length and spacing information from images and used
417 them to calculate RQD value. Li et al. [37] conducted research on the automatic
418 extraction of the discontinuity orientation, spacing, trace, roughness, and aperture,
419 which were used to calculate RMR and GSI. The other application of the extracted
420 discontinuity information is to analyze the stability of the surrounding rock mass of the
421 tunnel [28,33,34,63], which accounts for 13% of the subsequent analysis, as shown in
422 Fig.7 (b). Huang et al. [28] used the coordinates and orientations of joints to generate a
423 3D discrete model and investigate the stability of the surrounding rock of the tunnel;
424 their study results could guide the installation of tunnel supports. Zhu et al. [34]
425 integrated the 3D discontinuous deformation analysis (DDA) with DP to analyze the
426 stability of tunnels in blocky rock mass. The integrated system can support the high-
427 precision design of tunnels in construction. Similarly, Wang et al. [63] performed a 3D
428 stability analysis of tunnel blocks using the discontinuity information and the analysis
429 results provided a guidance for the adjustment of support parameters.

430 In addition to the discontinuity information, the extraction of water inflow [61]
431 information on the tunnel face during construction has also been studied. The
432 groundwater condition is a key parameter in the RMR system; therefore, after extraction

433 of the water inflow information, calculation of the RMR value was subsequently
 434 conducted, which could provide a basis for the determination of the support parameters.
 435 Moreover, some studies attempted to directly classify and characterize rock masses
 436 without calculating the RMR or other rating system values. Chen et al. [31] employed
 437 geological images of tunnel faces and a CNN to present an automated interpretation
 438 method for classifying five types of rock structures, including the mosaic, granular,
 439 layered, block, and fragmentation structures. The experimental results showed that the
 440 proposed method was optimal and efficient for automated classification of rock
 441 structures. Similar study has also been conducted by Qin et al. [64]. After classification
 442 of the rock mass structure, the support parameters can be determined accordingly.



443 Fig.8 (a) Proportion of extracted information from images in the reviewed literature.
 444 (b) Different subsequent analysis methods after the extraction of tunnel face data.

445 **4.2 Interpretation of TLS data**

446 Fekete and Diederichs [41] introduced a basic and general processing to interpret
 447 the point cloud data collected by TLS. The proposed workflow included 1) reducing
 448 the dataset to the zone of interest, 2) creating a surface model, 3) aligning with scans of
 449 previous face position or geo-reference to the absolute coordinate system, and 4)
 450 interpreting and extracting the data. Similar to the scan time, even based on the same
 451 processing workflow, the processing time of the point cloud data can significantly vary
 452 for different projects from 1 h [69] to several hours [39], depending on the chosen
 453 algorithm and size (up to GBs) of the point cloud data.

454 A brief summary of different categories of information extracted using TLS during
 455 the rock tunnel construction is presented in Table 2. Similar to DP, most of the

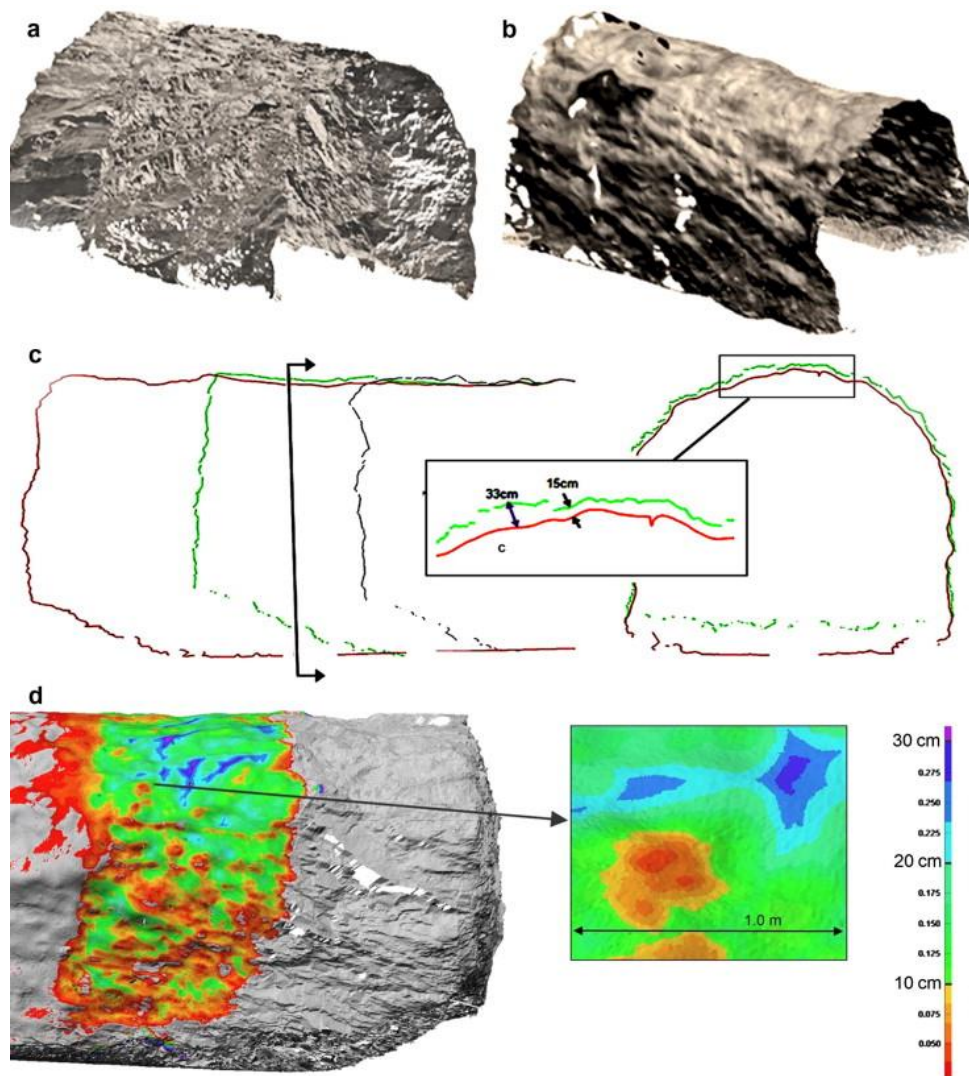
456 information extracted using TLS, including the dip, dip direction, spacing, roughness,
 457 trace length, and trace density, is related to discontinuity. In addition, the
 458 characterization of the rock mass and stability analysis of the tunnel system are the main
 459 applications of discontinuity information. Monsalve et al. [45] applied the extracted
 460 discontinuity information to characterize the rock mass and generated a discrete fracture
 461 network for each discontinuity set for further discontinuous modeling and calculation.
 462 Fekete et al. [41] integrated TLS with discontinuous modelling to analyze the stability
 463 of a tunnel in blocky rock mass, the result of which can influence the support scheme.
 464 Therefore, the usage of the extracted discontinuity using DP and TLS is similar.

465 Table 2 Examples of literature on different categories of the extracted information
 466 using TLS

Category	Detailed information	Refs
Discontinuity information	Orientation, location, spacing	[16]
	Dip, dip direction	[39]
	Location, orientation, joint set spacing, joint roughness	[41]
	Dip, dip direction, trace length, trace area	[45]
	Dip, dip direction	[69]
	Orientation, trace length, frequency, spacing, trace density	[70]
	Traces and orientations	[44]
	Dip, dip direction	[71]
	Discontinuity trace	[43]
Profile information	Tunnel profile geometry	[15]
	Support evaluation	[16]
	Tunnel deformation	[71]
	Overprofile, deformation of the shotcrete	[72]
	Overbreak, contour roughness	[73]

467 The other scenario where TLS-enabled information can contribute to the dynamic
 468 design of the tunnel support is to employ tunnel profile geometry information to
 469 evaluate or modify the support schemes. As presented in Table 2, several examples have
 470 been listed regarding this topic. Fekete et al. [16] used the scanned data to produce rock
 471 and final support profiles, where the rock face was scanned twice (pre- and post-
 472 shotcreting) to allow a direct comparison of the shotcrete thickness, as illustrated in
 473 **Fig.9**. The shotcrete thickness needs to be optimized if the comparison result is not

474 acceptable or an overbreak is detected. Kim and Bruland [73] proposed Tunnel Contour
475 Quality Index (TCI) based on TLS for the effective management of tunnel contour
476 quality, whose roughness can affect the shotcrete volume or rock bolts. In the studies
477 carried out by Xu et al. [71] and Walton et al. [72], deformation of the excavated section
478 and as-built shotcrete thickness were detected using TLS, the time spent was relatively
479 long, that is, about one month. It should be noted that they do provide valuable
480 instructions on the optimization of the support schemes; however, they are beyond the
481 scope of the study due to the long acquisition time. Such is also the case in some
482 literature using long-term monitoring results of the as-built tunnel structure, as
483 mentioned above in Section 2.



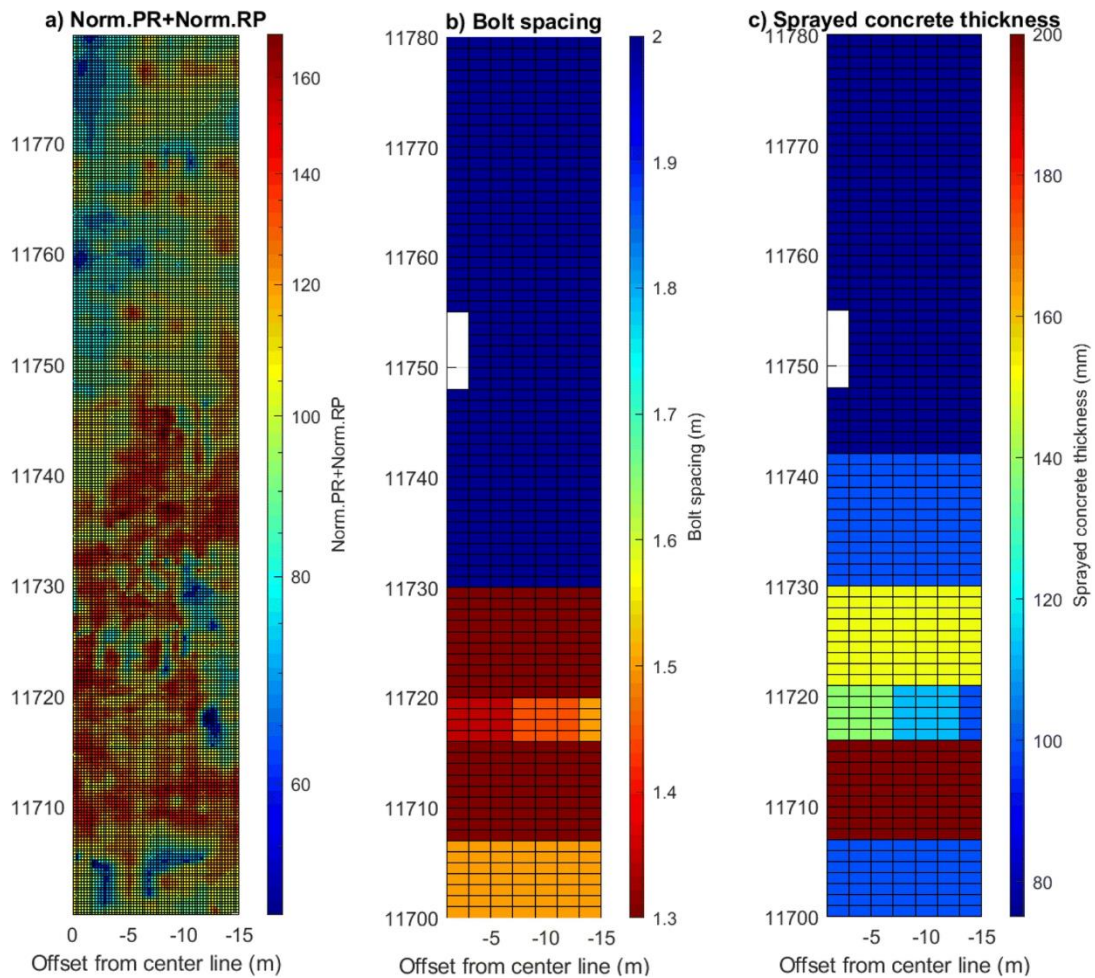
484
485 Fig.9 (a) Rock model. (b) Shotcrete Lidar model. (c) Longitudinal and cross-section
486 showing detailed comparison of profiles with shotcrete thickness. (d) Shotcrete

487
488
489
490
491
492
493
494
495
496
497
498
499
500
501
502
503
504
505
506
507

thickness contoured onto rock model [16]

4.3 Interpretation of MWD data

One of the most widespread applications where MWD data contribute to the dynamic design of the support during tunnel construction is to characterize the rock mass and provide support parameters accordingly (see Table 3). A case study was reported by Galende-Hernandez et al. [74] where ten kinds of MWD variables, including the penetration rate, hammer pressure, water pressure, and seven other variables, were processed and analyzed using machine learning and computational intelligence techniques to estimate the RMR value. The results were applied to a D&B tunnel and exhibited a satisfactory performance. Similarly, van Eldert et al. [75] used MWD fracturing index (FI) to characterize the rock mass for grouting purposes. However, neither of the studies mentioned the design of the support in the context, nor directly determined the relationship between the rock mass grade and support parameters. To establish correlations between MWD data and installed rock support, van Eldert et al. [1,2] correlated the weighted normalized penetration rate and rotation pressure with the RQD and Q values. Subsequently, the normalized penetration rate and rotation pressure were employed to predict the rock support parameters (bolt spacing, bolt length and concrete thickness), as illustrated in **Fig.10**. The results were compared with those of the Q-value-based method, which exhibited a reasonable correlation. Therefore, the FI value can be used as an indicator to predict the rock support.



508

509

Fig.10 (a)-(c): Visualizations of the MWD parameters, bolt spacing and sprayed concrete thickness [2]. (PR: penetration rate, RP: rotation pressure)

510

511

512

513

514

515

516

517

518

519

520

In addition to the characterization of the rock mass, another key application of the MWD data to assist the support design is to detect the potential overbreak zones. Navarro et al. [50] developed a nonlinear multivariable model to predict the excavated mean distance and lookout distance as functions of the normalized penetration rate, rotation speed, hammer pressure, water flow, and rotation pressure parameters. The predicted excavated mean and lookout distances can be considered as a damage measure to predict the high risk of potential over- or under-excavated zones produced by blasting in the contour of a tunnel, thus reinforcing the support if necessary.

Table 3 Examples of literature on different usages of the MWD-enabled data during tunnel construction

Category	Details	Refs
----------	---------	------

Rock mass characterization	Calculation of RQD and Q value to determine the bolt spacing and concrete thickness	[1]
	Calculation of FI and investigation of relationship with Q system to predict bolt length, bolt spacing and concrete thickness	[2]
	Estimation of RMR value	[74]
	Calculation of FI	[75]
Overbreak zone detection	Prediction of the excavated mean distance and the lookout distance	[50]

521

522 **4.4 Interpretation of other ahead geological prospecting data**

523 Processing the acquired raw data using the geological prospecting technologies
524 depends on the computational power of the computer, specific software, processing
525 algorithm and size of the data. According to the interviewed domain experts and
526 engineers, data processing can be accomplished in 2 h. As for the acquired data by
527 ahead geological prospecting technologies and its contribution to the dynamic design
528 of the tunnel support, a brief summary of the application of ahead geological
529 prospecting techniques in timely data interpretation during tunnel construction is given
530 in Table 4. Using the high-frequency electromagnetic pulse, GPR satisfactorily
531 responds to rock structures, such as faults, lithological interfaces, and fracture belts [76].
532 Hence, some studies were conducted using GPR to detect seismic and nonseismic
533 geological features [77], karst geological anomalies [78], and the position and shape of
534 catastrophic geological body [79]. Based on the detection result, the original support
535 schemes can be modified. In addition, Qin et al. [80] introduced an automatic
536 recognition method to directly identify steel ribs, voids, and initial linings from GPR
537 images using CNN methods to control the quality of the support, which is a critical
538 issue in guaranteeing the safety of both tunnel structures and construction operations.

539 In contrast to GPR, TSP exploits seismic waves that are excited by small-scale
540 artificial blasting to predict unfavorable geology conditions. Parameters of the seismic
541 waves include the longitudinal wave (P-wave) velocity, transverse wave (S-wave)
542 velocity, magnitude of the wave, wave type, wave depth, wave direction and so on, as

543 shown in Table 4. One of the key applications of TSP-based data is the classification
 544 and characterization of rock masses. Bu et al. [81] used P-wave velocity, as well as
 545 Poisson's ratio and Young's modulus, to classify the rock mass ahead of the tunnel face
 546 into 5 grades. Shi et al. [82] combined P- and S-wave velocity with Poisson's ratio and
 547 Young's modulus to classify the rock mass using the fuzzy analytic hierarchy process
 548 method. Moreover, the calculation of the RMR value of the rock mass using TSP data,
 549 e.g. P- and S-wave velocity, wave magnitude, wave depth and direction, has been
 550 carried out by several studies [83-85], where the rock bolts, shotcrete and steel sets can
 551 be determined directly according to the different RMR values. In addition to the
 552 characterization of rock masses, TSP has also been integrated with stability analysis to
 553 provide a guidance for support design. Fan et al. [86] conducted the discrete element
 554 method (DEM) to analyze the deformation and displacement of the rock mass using the
 555 discontinuous geological interface information collected by TSP. The analysis results
 556 could have practical guiding significance for the design of the support.

557 Comprehensive prospecting methods have been proposed and applied in
 558 construction because each prospecting technique has its advantages and disadvantages.
 559 Cao et al. [87] determined the support type and method dynamically during tunnel
 560 construction based on the TSP and GPR data. After the detection of well-developed
 561 structure planes, such as faults and folds, along with the abundant water, steel frame,
 562 steel meshes, and shotcrete thickness were optimized accordingly. Bu et al. [76] and
 563 Nie et al. [88] combined GPR and TEM to detect the position and spatial distribution
 564 pattern of water-rich areas. These results provide an effective reference for the
 565 implementation of dynamic design and construction schemes.

566 Table 4 Summary of ahead geological prospecting techniques in data acquisition

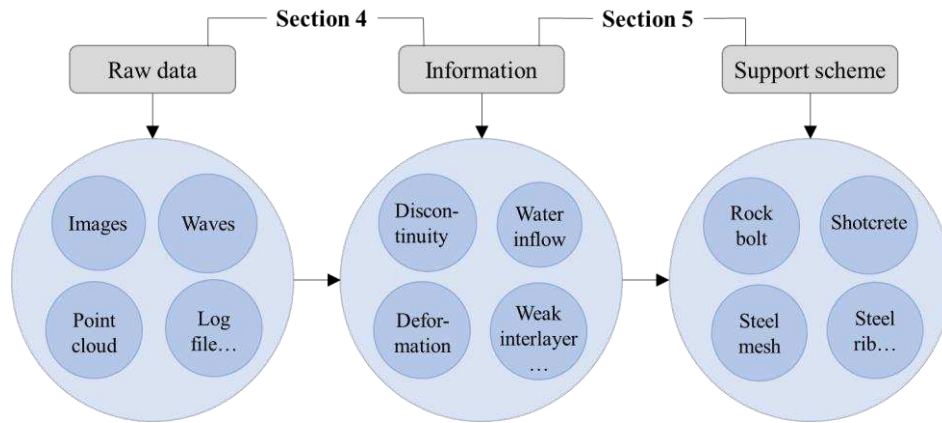
Techniques	Detected data		Contribution	Refs
GPR	Seismic	and non-seismic	NA	[77]
	geological features			
	Different types of karst geological anomalies		NA	[78]
	Steel ribs, voids, and initial linings		Quality control of the support	[80]

	Position and shape of catastrophic geological body	NA	[79]
TSP	P- and S-wave velocity ratio, Poisson's ratio, Young's modulus	Classification of the rock mass	[81]
	P- and S-wave velocity ratio, Poisson's ratio, Young's modulus	Classification of the surrounding rock mass	[82]
	Discontinuous geological interface information	Stability analysis of the surrounding rock	[86]
	Unstable ground conditions	Calculation of RMR value	[83]
	P- and S-wave velocity, wave magnitude, wave depth, direction	Calculation of RMR value	[84]
	P- and S-wave velocity, wave magnitude, wave depth, direction	Calculation of RMR value	[85]
GPR, TSP	Faults, folds, groundwater	Modification of steel frame, steel meshes, shotcrete thickness and bolt	[87]
GPR, TEM	Position and spatial distribution pattern of the water-rich area	NA	[76]
GPR, TEM, ER	Weathered area	NA	[88]

567

568 **5 Data aggregation for support parameters determination**

569 Sections 3 & 4 focus on the quick acquisition of the data on the construction site
570 and the corresponding interpretation, such as the interpretation of rock mass parameters
571 from images and interpretation of geological anomalies from the TSP waves. Although
572 some studies examined the corresponding aggregation of the interpretation results, such
573 as the calculation of RMR, this study attempted to simplify the process from the
574 interpretation results to support schemes. With the increasing development of IT,
575 multiple computer- and AI-aided aggregations have been applied to optimize support
576 schemes from multiple sources of data. Here, another key issue of the dynamic design
577 of rock tunnel supports, that is, the efficient aggregation of the data exposed by
578 excavation using computer- or AI-aided methods, is discussed. The relationship
579 between Section 4 and Section 5 are shown in **Fig.11**.



580
581 Fig.11 Relationship between Section 4 and Section 5

582 **5.1 Conventional methods**

583 Generally, three traditional methods are mainly used in the determination of the
584 tunnel support parameters: empirical, numerical and analytical methods [89,90]. The
585 empirical method refers to the determination of the design parameters based on the pre-
586 existing standard methods or pre-existing experience [6], which can be quantified by
587 rock mass classification systems such as afore-mentioned RMR and Q value. Upon the
588 classification of the newly exposed rock mass, the corresponding support parameters
589 can be determined. Some examples of using rock mass classification systems to
590 determine support parameters have been discussed in Section 4.

591 Numerical methods employ both the computational hardware and software to
592 evaluate the rock mass behavior and its effects on the support systems, including the
593 finite element method (FEM) and DEM. Due to its ability to simulate the stresses and
594 deformations that develop in the support system, it has become a powerful and widely
595 used tool to design rock tunnel support [18]. Sopacı and Akgün [91] used a 2D FEM
596 program to analyze the total induced displacement and percentage of yielded elements
597 of the tunnel; the results were used to optimize the empirically determined support
598 parameters. Similarly, Kanik et al. [92] applied a 2D FEM software to calculate the
599 thickness of the plastic zone and total displacements of the tunnel, whose supports were
600 estimated using both RMR_{14} and RMR_{89} . According to the analysis results, as shown
601 in **Fig.12**, the support systems obtained from the RMR_{14} version suggests more realistic
602 support element for fair rock masses and great horizontal stress values. In the study

603 carried out by Aygar and Gokceoglu [93], NATM principles were entirely reflected in
 604 the calculations and the input parameters of the numerical models were the
 605 interpretation results of the geotechnical monitoring task performed during the
 606 construction. Total displacements, vertical displacement, horizontal displacement and
 607 the yielding zone were calculated using 2D FEM methods to get the optimal support
 608 system.

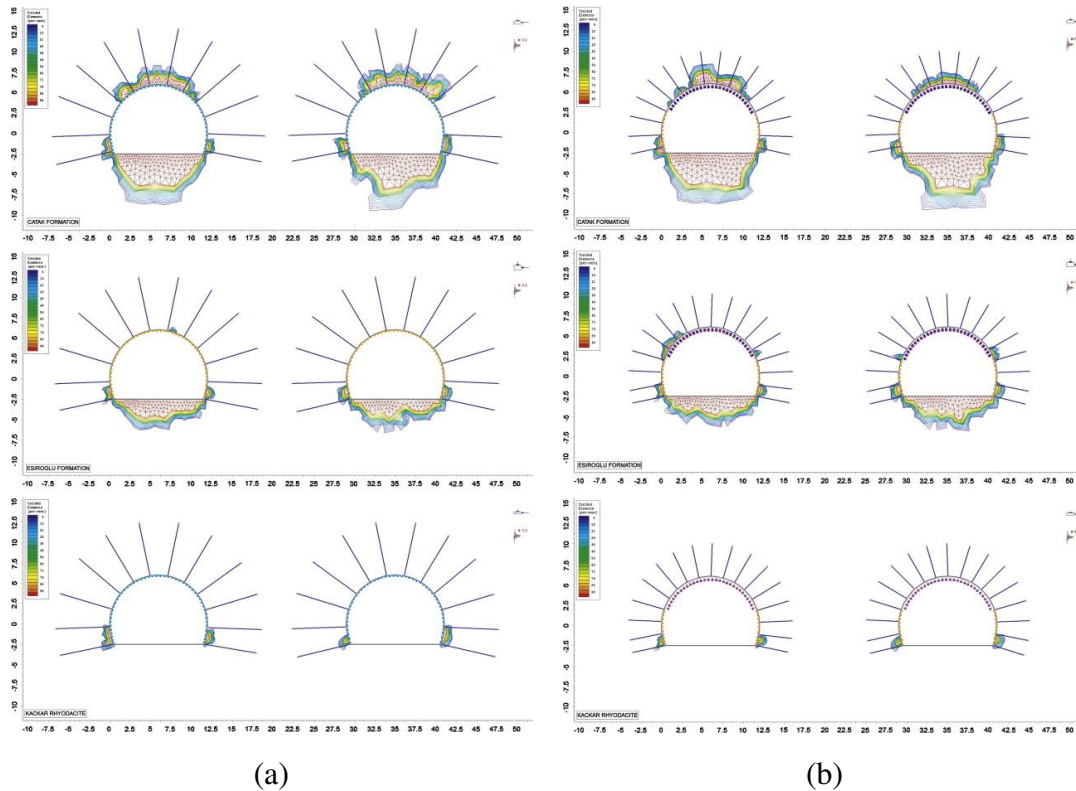


Fig.12 Thickness of plastic zone after installation of support systems suggested by:

(a) RMR₁₄; (b) RMR₈₉. [92]

609 However, 2D numerical methods can not accurately solve the support optimization
 610 problem as in essence, the support optimization problem is a mechanical problem with
 611 three-dimensional effect. The comparison study conducted by Kaya and Sayin [90]
 612 revealed that 3D FEM analysis gave the better solution in tunnel support design
 613 compared to 2D FEM analysis. Hence, 3D numerical analysis has been carried out by
 614 many researchers regarding tunnel support design. Theoretically, Zhang and Zhu [94]
 615 proposed a 3D version of the Hoek-Brown strength criterion, i.e. generalized Zhang-
 616 Zhu (GZZ) strength criterion, which considered the intermediate principal stress

617 compared with the original 2D Hoek-Brown strength criterion. Based on the GZZ
618 strength criterion, Xu et al. [95] used analytical and numerical methods to investigate
619 the interaction between tunnel support and surrounding rock and predict the
620 deformability of the surrounding rock. With the advancement in the numerical software,
621 many research endeavors have been allocated to 3D numerical analysis based on this
622 approach. Feng et al. [9] and Xing et al. [96] used the 3D numerical analysis to get the
623 optimal length and spacing of the rock bolt, and investigate the displacements and
624 stresses of the tunnel, respectively. Hsiao et al. [97] used the computer program FLAC-
625 3D to simulate the tunnel construction and the numerical results were used for support
626 optimization. In the study carried out by Sun et al. [98], the surrounding rock stress
627 release rate was considered in the calculation to obtain the stability of tunnel lining
628 support, which was also implemented in FLAC-3D. In terms of the time consumed, the
629 computational time of the numerical analysis depends on many factors such as mesh
630 numbers and mesh size, ranging from several minutes to several hours.

631 Last but not least, analytical methods that use mathematical and mechanical tools
632 to calculate the stress distribution state of the surrounding supported or unsupported
633 rock are widely used in the design of rock tunnel supports. Compared with the
634 numerical methods, analytical methods rely on a number of assumptions and
635 simplifications to formulate the analysis, therefore are simpler, more intuitive, and
636 computationally efficient [18,99]. Su et al. [100] used convergence confinement
637 method (CCM), which is a useful and effective analytical method to simulate the
638 mechanical behavior of the rock mass during tunneling and analyze the stability of the
639 tunnel and its supports. The results provide a guidance for the optimization of the rock
640 bolts and shotcrete parameters, such as elasticity modulus, diameter, longitudinal
641 spacing, bolt length, Young's modulus, Poisson's ratio, bending strength, and shotcrete
642 thickness. To overcome the limitation of hydrostatic loading simplification that CCM
643 may encounter in the tunnel support design, Mitelmam and Elmo [18] adopted
644 equivalent boundary beam (EBB) method to readily compute the distribution of field

645 stresses between the ground and support system, the results of which were used to
 646 optimize the lining thickness and rock bolt. In this study, the comparison between the
 647 efficiency of the proposed EBB method and the efficiency of the FEM method was also
 648 conducted. The results for the proposed EBB method were generated almost
 649 instantaneously while the simple FEM models would take about 10 min to be setup and
 650 calculated. Hence, it can be seen that in some simple and simplified situation, analytical
 651 methods outperform other methods from the perspective of computational efficiency.

652 **5.2 AI-supported methods**

653 Conventional methods are appropriate candidates for designing tunnel support
 654 when the available data for projects are sparse [20]. However, the increasing amounts
 655 of data collected from the construction site are posing a challenge to conventional
 656 analysis methods as the accuracy and efficiency are easily affected [20]. Herein lies an
 657 opportunity to integrate AI methods into the existing best practices of the rock tunnel
 658 support design to make the best use of the large amount of data, as AI can solve complex
 659 engineering problems by learning patterns of data inputs and outputs presented to the
 660 models to produce meaningful interpretation [101]. Hence, AI is gaining momentum in
 661 the design of rock tunnel support, and different AI techniques have been used in the
 662 literature, such as artificial neural network (ANN) [102-105], genetic algorithm (GA)
 663 [106-108], particle swarm optimization (PSO) [104,109,110], support vector machine
 664 (SVM) [111,112] and so on. For these techniques, the development of the principles
 665 and of the mathematic models have been introduced and discussed in the existing
 666 studies [101,113], which therefore are excluded in this subsection. Details of the
 667 application of AI in the design of the support from the collected literature are
 668 summarized in Tab.5.

669 Table 5 Applications of AI techniques in the design of the rock tunnel support

Refs	AI techniques	Description of applications
[114]	Expert system, Fuzzy set	Prediction of rock bolt, shotcrete, wire meshes parameters
[108]	GA, SVM	Classification of BQ value
[109]	PSO	Optimization of anchoring parameters

[106]	GA	Optimization of steel rib supports
[111]	SVM	Selection of pre-determined support patterns
[115]	SVM, ANN	Calculation of shotcrete thickness, diameter of bolt, and length of bolt
[103]	ANN	Selection of one of the support patterns from 6 pre-determined patterns
[110]	SVM, PSO	Optimization of shotcrete thickness and shotcrete Young's modulus
[107]	GA, SVM	Prediction of RMR value
[112]	SVM	Classification of surrounding rock mass
[104]	ANN, GA, PSO	Characterization of rock mass quality
[105]	ANN	Establishment of relationship between rock quality and support parameters
[116]	Neuro-fuzzy inference system	Prediction of RMR value
[117]	Expert system, machine learning	Establishment of relationship between rock mass quality and support parameters
[102]	ANN	Prediction of shotcrete, rock bolt, steel mesh, steel arch and advanced small pipe
[118]	Expert system, ANN, Case-based reasoning	Prediction of shotcrete, rock bolt, and steel mesh
[119]	Expert system	Prediction of rock bolt, steel mesh and shotcrete

670 It can be seen from Table 5 that one of the scenarios where AI is applied to solve
671 support design problem is, likewise, the characterization of the rock mass, which is used
672 as the indicator of the corresponding support parameters. Liu et al. [108] introduced GA
673 and SVM coupling algorithm to get the improved BQ value. Similarly, Gholami et al.
674 [107] and Wang et al. [112] also used SVM to predict the RMR value of the rock mass
675 and classify the surrounding rock in a timely manner, respectively. In addition to SVM
676 method, Liu et al. [104] used ANN model to predict the rock mass quality using MWD
677 data and Sebbeh-Newton et al. [116] adopted neuro-fuzzy inference system to predict
678 basic RMR value using on-site data. None specific study reported the time used but it
679 can be speculated that the process to get the results using these AI techniques is timely
680 as it has provided real-time assistance for design alternations in the construction site
681 [112].

682 Other studies listed in Tab.5 focus on the direct optimization or selection of
683 support patterns without classifying rock mass. Global optimization algorithms such as

684 PSO and GA are used by Li et al. [109] and Alvarez-Fernandez et al. [106] to optimize
685 the anchorage and steel rib parameters respectively, where little computational cost was
686 needed as the implementation of both GA and PSO is easy and simple. The second type
687 which is usually used in the literature to directly optimize the support parameters is the
688 classification model such as SVM. For example, Liu et al. [115] used 16 factors such
689 as density of joint and discontinuity orientation as input variables of SVM network to
690 get the shotcrete thickness, diameter, length and spacing of rock bolt, diameter and
691 spacing of wire mesh. SVM was also integrated with numerical analysis and PSO by
692 Jiang et al. [110] to represent the nonlinear relationship between the surrounding rock
693 mechanical parameters and displacements, which provided a real-time and quantitative
694 approach to optimize shotcrete parameters.

695 Given the advantage of computing a mapping from a multivariate space of
696 information to another [120], the ANN model is thus widely used in the support design
697 to describe the end-to-end relationship between rock parameters and support parameters.
698 ANN model has superiority in the support design problem as it is able to consider
699 qualitative descriptive information in tunnel design problems such as rock grade and
700 weathering grade, and the applied data can be imperfect and erroneous [102]. Xia et al.
701 [102] introduced ANN method into tunnel support design earlier and verified the
702 feasibility and reliability of ANN-supported support design. Using 9 parameters
703 including geological factors, tunnel width and buried depth as inputs, 13 kinds of
704 support parameters were outputted by ANN. Similarly, Nie et al. [105] mapped the
705 relationship between rock conditions, the sequential excavation parameters and support
706 parameters using ANN. The results illustrates the feasibility of the proposed ANN-
707 based design method with much less computing time compared with numerical
708 methods. In a different way, Liu et al. [103] explored the correlation between MWD
709 data and support patterns using ANN and found that a neural network with a 6-30-6
710 topology structure was optimum, whose calculation time was approximately 10 min.
711 The calculation result was to select one of the support patterns from 6 pre-determined

712 patterns.

713 Last but not least, expert system is also adopted by many researchers to solve the
714 support design problem, as a large amount of historical data and cases within the scope
715 of tunnel support design exist. As early as the last century, Madhu et al. [114]
716 constructed an expert system using rule-based reasoning, i.e., knowledge being
717 represented as “if-then” rules in the system. Data uncertainty was treated using a fuzzy
718 set analysis. The application of the expert system elucidated that the recommended rock
719 bolt, shotcrete and wire mesh parameters were in line with those actually used. Similarly,
720 Wang et al. [119] constructed an expert system which took into account 8 factors such
721 as joint orientations and water inflow information. Later, many researchers endeavor to
722 integrate expert system with other techniques to enhance the robustness and improve
723 the accuracy of the established expert system. Wang [117] combined expert system with
724 machine learning to get the support parameters from 5 types of input data including
725 buried depth, tunnel face stability grade, surrounding rock grade and others. Qiao and
726 Wei [118] integrated expert system with ANN and case-based reasoning to avoid the
727 bias that a single method is prone to. Using this comprehensive method, the shotcrete,
728 rock bolt and steel mesh parameters were determined and were close to the ones in
729 practice.

730 **6 Conceptual framework of JIT design of rock tunnel support**

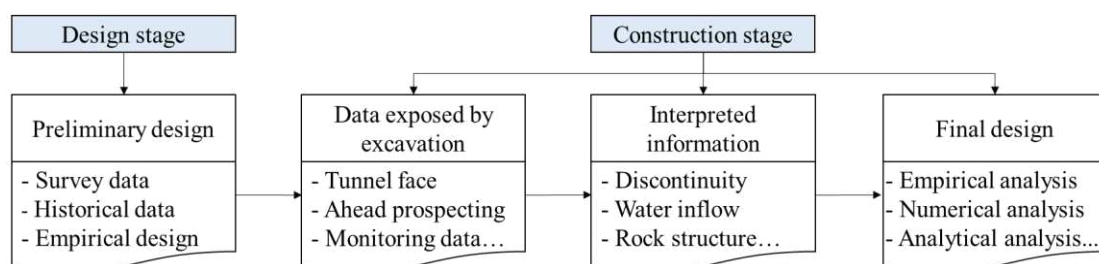
731 According to the reviewed studies, the advancement of IoT and IT technologies
732 has improved the performance of support design tasks in the rock tunnel construction
733 concerning the time and accuracy. Here, a brief definition and overview of the proposed
734 conceptual framework are presented, and research gaps are identified accordingly.
735 Subsequently, the conceptual framework for the JIT design of tunnel supports,
736 including key concepts and future perspectives, is developed.

737 **6.1 Framework definition and overview**

738 The existing academic and industrial-based studies have proved that an accurate,
739 safe, and particularly JIT design of rock tunnel supports can fulfill the safety, stability,

740 and other requirements for certain underground conditions [3,10,11]. The “just-in-time”
 741 concept originates from the manufacturing workflow with an aim to reduce the flow
 742 time and costs of production systems and distribution of materials [121], and then has
 743 been introduced into computer science industry. For instance, a JIT compiler is used to
 744 improve the runtime performance, which gives an equivalent sequence of the native
 745 code as soon as the bytecode sequences are given [122]. Similarly, here, we use the
 746 term “just-in-time” to denote the intrinsic requirement of the rock tunnel support as the
 747 support parameters need to be determined as soon as the hidden volume of the rock
 748 mass, the structural surface, the underground water and the mechanical response of
 749 surrounding rock, are exposed during tunnel construction. The JIT design of the tunnel
 750 support implies that once the data during construction are available in time, the revision
 751 of the preliminary design can also be available in time. Hence, in the JIT design of the
 752 tunnel support, data acquisition, interpretation and aggregation all need to be in time.

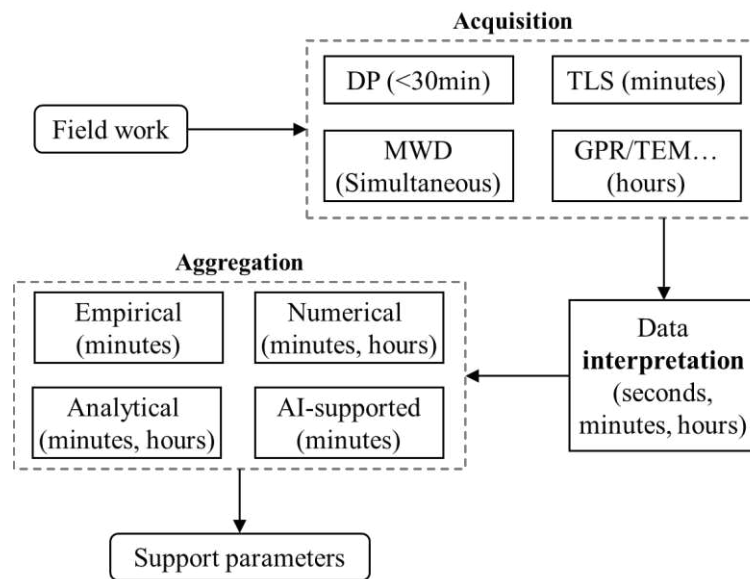
753 The flowchart of the dynamic design of the support can be seen in **Fig.13**. It can
 754 be seen that the dynamic design of the tunnel support focuses on the revision of the
 755 preliminary design using the exposed geological and various unanticipated conditions
 756 during the construction process. By comparison, the JIT design of the tunnel support is
 757 a higher requirement for the dynamic design of the tunnel support, that is, as mentioned
 758 above, the revision of the tunnel support schemes should be available in time as soon
 759 as the new data are available during the construction process.



760
761 Fig.13 Flowchart of dynamic design of the support in rock tunnel

762 In this paper, we provide a broad overview of currently state-of-the-art techniques
 763 used in the design of the tunnel support during tunnel construction. In previous sections,
 764 the contribution of each technique to the JIT design of the rock tunnel support was

765 thoroughly discussed. A brief summary of the workflow and average time requirements
 766 for the support design in the current practice is given in **Fig.14**.



767

768 Fig.14 Workflow and average time requirements for support design in current
 769 practice.

770 To sum up, the optimization of the support schemes during rock tunnel
 771 construction can be divided into three steps, i.e., acquisition of on-site raw data,
 772 interpretation of the data and the aggregation of the interpretation results to obtain new
 773 support schemes. As discussed in Sections 4 and 5, one of the key parameters that we
 774 consider in the process of JIT design of the tunnel support is the time required to
 775 accomplish the task. It can be seen that the time it takes to accomplish each step is
 776 closely related to the size of the tunnel face, IoT technique employed to acquire data,
 777 and IT technique used to analyze the information, ranging from several seconds to
 778 several hours. For instance, generally, it takes less than 30 min for DP to collect on-site
 779 data [30] while it may take more than 1 h for TSP to acquire data, as illustrated in **Fig.14**.
 780 In addition to time consumption, other important factors that may influence the
 781 performance of the JIT design of the tunnel support, such as the information category
 782 and algorithm accuracy, have also been discussed. There exist some parallels in the
 783 techniques used in each step. As can be seen from Section 4 and 5, the dominant
 784 information that each technique extracts from raw data is the discontinuity information,

785 followed by profile information. Then, the majority of the literature samples use these
786 information to conduct rock mass characterization and stability analysis, based on
787 which the support parameters can be determined accordingly.

788 **6.2 Research gaps**

789 Three major shortcomings of current JIT design of the tunnel support have been
790 identified from the literature examples, which are discussed in detail below.

791 **6.2.1 High time consumption of data interpretation**

792 The application of IoT technologies, including DP, TLS and MWD technologies,
793 has enabled the quick acquisition of on-site data, which is the foundation of the JIT
794 design of the tunnel support. However, the corresponding interpretation of the collected
795 raw data may consume a considerable time in some cases, which is typically illustrated
796 in the interpretation of the point cloud data. With a triangular mesh size of 4 cm and
797 382,085 facets, the interpretation of the point cloud takes about 2.5h in a workstation
798 (the Intel Core i7-2600 CPU and 16GB RAM) [54]. To interpret the point cloud data
799 with the recommended resolution of 7.5mm at 5 m, the processing time of the point
800 cloud was approximately 5 h [39]. The time to process high-density point cloud data in
801 some cases can exceed 20 h, even with a high-powered computer (Intel Core i7-6700
802 CPU and 16GB RAM) [32]. In addition to the interpretation of point cloud data, the
803 processing of digital images can also take a high computational time, as seen in [28]
804 where 1.5 hours were needed for post-processing. The relatively high time cost can
805 hinder the performance of the JIT design of the tunnel support as the intrinsic quick-
806 response requirement cannot be guaranteed.

807 **6.2.2 Dilemmas of conventional and AI-supported aggregation methods**

808 Empirical, numerical and analytical approaches are the dominant methods which
809 are used in practice to obtain the optimal support parameters. However, through
810 literature examples, some limitations have been identified that can pose challenges to
811 the JIT design of the tunnel support.

812 **(1) Limitation of empirical classification approaches**

813 As discussed, the majority of the literature used the extracted discontinuity or
814 water inflow information to characterize the rock mass, then gave the support scheme
815 from the predefined schemes. This is a one-to-one process, i.e., one class of surrounding
816 rock mass corresponds to a specific type of support parameters. As can be seen from
817 Table 6, the one-to-one relationship between the RMR values and corresponding
818 recommended types of support in a practical tunnel project is obvious [123]. This
819 common practice simply produces a qualitative ranking process for the rock mass and
820 neglects the stresses or deformations that develop in the support system [18], which
821 therefore tends to yield inaccurate and resource-wasting support schemes. Indeed, the
822 newly exposed data, such as the discontinuity information, can be used to not only
823 characterize the rock mass but also to quantitatively evaluate the entire support-rock
824 system stability (see [34]), whose result can be used as an indicator to optimize the
825 support parameters in detail. Unfortunately, most studies using the empirical
826 classification method fail to further integrate the on-site information with more precise
827 analysis methods to improve the accuracy of the JIT design of the tunnel support.

828 Table 6 Recommended types of support based on RMR system [123]

RMR value	Anchoring Φ 20mm	Shotcrete	Ribs
81-100	-	-	-
61-80	Locally bolts in crown, 3m long, spaced 2.5m, with occasional wire mesh	50 mm in crown where required	-
41-60	Systematic bolts 4m long, spaced 1.5-2 m in crown and walls with wire mesh in crown	50-100 mm in crown, 30 mm in sides	-
21-40	Systematic bolts 4-5 m long, spaced 1-1.5 m in crown and walls with wire mesh	100-150 mm in crown, 100 mm in sides	Light ribs spaced 1.5m where required
<20	Systematic bolts 5-6 m long, spaced 1-1.5 m in crown and walls with wire mesh. Bolt invert	150-200 mm in crown, 150mm in sides and 50 mm in face	Medium to heavy ribs spaced 0.75m with steel lagging and fore poling if required. Close invert

829 **(2) Shortcomings of numerical and analytical approaches**

830 The limitations of empirical methods do not apply to numerical and analytical

831 approaches; thus, both the numerical and analytical approaches have been widely used
832 in practice to improve the accuracy or efficiency of the computation. However, the
833 numerical analysis of the support parameters is sensitive to the mesh and boundary
834 effects, which may require considerable time to yield results [96]. Moreover, the
835 modelling process of numerical analysis can also be time-consuming as various factors
836 need to be taken into account. In comparison, analytical approaches provide a simpler
837 and more computationally efficient way to aggregate data with various simplified
838 hypotheses, which, in turn, limits the application of analytical methods as the simplified
839 conditions are seldom the case in most rock tunnel problems [96].

840 **(3) Scarcity of the AI-supported methods**

841 The use of AI techniques, such as optimization algorithms, ANN and expert
842 system, has greatly improved the performance of the JIT design of the tunnel support
843 concerning the computational time [105] and accuracy [20]. Contrary to our initial
844 expectation that many studies were conducted on the AI-supported JIT design of tunnel
845 supports, actually, only 12 literature using AI to directly optimize support parameters
846 were collected, excluding the studies that used AI to classify the rock mass. Moreover,
847 Published between 2002 and 2005, four of these studies [102,115,118,119] used ANN
848 and an expert system to find the optimal support parameters. Consequently, AI has been
849 widely adopted in the entire process of the JIT design of tunnel supports, such as
850 interpretation of on-site raw data. In addition, it is a powerful tool to describe the end-
851 to-end relationship between the rock and support parameters [120]; however, studies
852 that directly use AI to establish relationships between newly exposed data and support
853 parameters are scarce.

854 **6.2.3 Long retrieval time for similar design cases**

855 According to the current standards and specifications [10,11], the pre-existing
856 experience or cases of rock engineering support design can be reused if the new tunnel
857 project encounters similar geological conditions as before. Therefore, it challenges
858 designers/engineers to recall and search past similar projects and extract associated

859 information [118]. This process is subjective and error-prone, as designers/engineers
860 rely on their own experience and comprehension to retrieve and edit similar cases.
861 Moreover, manual retrieval is time-consuming; therefore, some researchers have
862 attempted to use computer-aided approaches to improve the accuracy the efficiency of
863 the process (see examples in [117,118]). However, the concerns that how to convert the
864 textual cases or knowledge into computer-interpretable data formats and how to retrieve
865 the cases accurately still have not been fully addressed, which influences the
866 performance of the JIT design of the tunnel support.

867 **6.3 Key concepts**

868 Three key performance indicators that can be used to evaluate the performance of
869 the JIT design of tunnel supports during the rock tunnel construction process are
870 discussed.

871 **(1) Time consumption**

872 Support is installed during the construction process after the face is excavated, and
873 the muck is loaded. According to engineering experience, the time for “acquisition-
874 interpretation-aggregation” of the support design is extremely limited [16] as mucking
875 and risk removal can consume approximately 2-3 h, accounting for over 50% of the
876 cycle time; thus, the time allocated to the support design is only approximately 1 h.
877 Hence, under such circumstance, the JIT design of the tunnel support requires the
878 “acquisition-interpretation-aggregation” workflow to be finished within 1 h. Otherwise,
879 the working hours can be increased and the overall construction period can be easily
880 delayed. However, as stated in Section 6.2, in certain cases, some design approaches
881 fail to meet the “time” requirement of the JIT design of the tunnel support.

882 **(2) Accuracy**

883 Inaccurate support parameters adversely affect the safety guarantee in poor rock
884 mass conditions and waste both the support structures and manpower in fair rock mass
885 conditions. As the JIT design of the tunnel support consists of “acquisition”,
886 “interpretation” and “aggregation”, the accuracy of the JIT design of the tunnel support

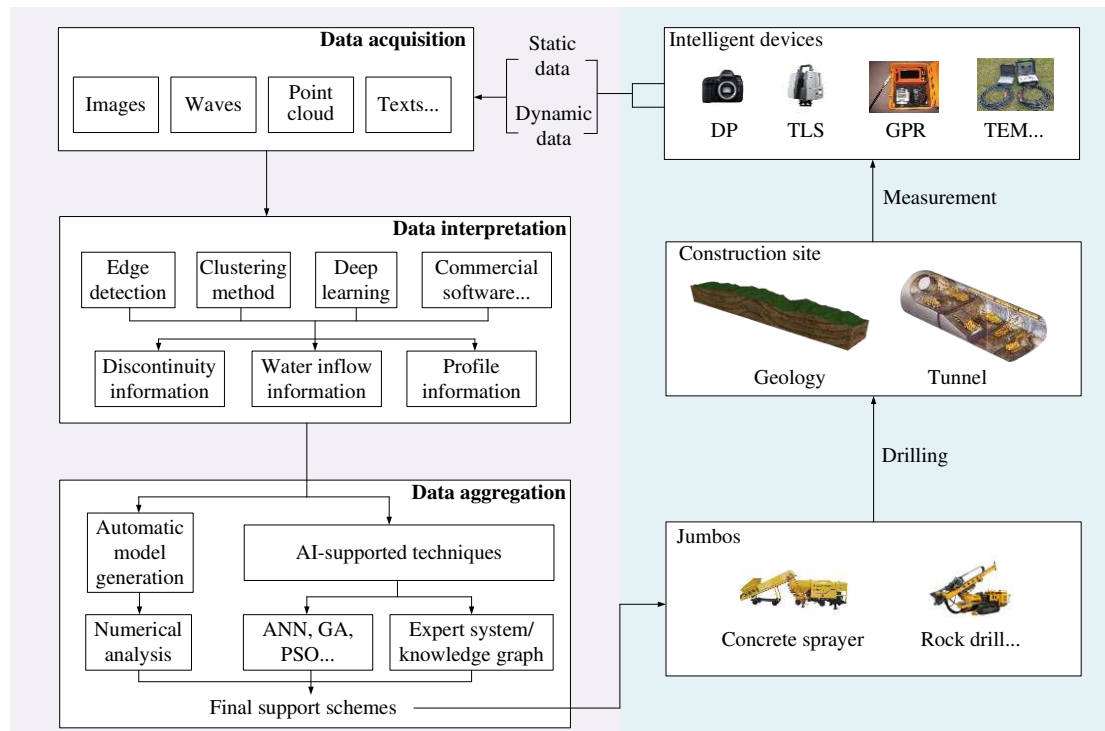
887 can be explained by many aspects, such as the resolution of the acquired data [16] and
888 the accuracy of the interpretation [61] and aggregation [103] algorithms. That's to say,
889 higher-resolution data, as well as more appropriate and accurate interpretation and
890 aggregation methods, tends to improve the performance of the corresponding JIT
891 design of the tunnel support.

892 (3) Degree of automation

893 Automation in the support design is composed of many aspects in the “acquisition-
894 interpretation-aggregation” workflow, such as the application of automatic machinery
895 [47], automatic model generation [32], automatic information extraction [17,53,54] and
896 automatic information aggregation [117]. The degree of automation significantly
897 affects the performance of the JIT design of the tunnel support. For instance, one of the
898 primary difficulties in the implementation of discontinuous numerical methods for rock
899 mass is generating discontinuous models [34]. If the model is generated automatically
900 and accurately, the overall computational efficiency shall be greatly improved. Hence,
901 higher degree of automation can, to some extent, improve the performance of the JIT
902 design of the tunnel support.

903 6.4 Conceptual framework and future perspectives

904 Considering the time, accuracy and automation requirements of the JIT design of
905 the tunnel support, a conceptual framework for the JIT design of the tunnel support is
906 presented in **Fig.15**. The entire framework considers the pros and cons of each
907 technique used in the “acquisition-interpretation-aggregation” workflow. The left part
908 of **Fig.15** shows the workflow of the “acquisition-interpretation-aggregation”, whose
909 relationship with the construction site is presented in the right part.



910

911 Fig.15 Conceptual framework for JIT design of the tunnel support during rock tunnel
 912 construction

913 Using intelligent acquisition methods such as DP, TLS and GPR, on-site data can
 914 be collected in various forms. Then, based on the efficient and accurate methods
 915 presented in Section 4, e.g. edge detection and deep learning, the discontinuity, water
 916 inflow and profile information can be interpreted. In the third step, the information is
 917 used as inputs to automatically generate numerical models or obtain support parameters
 918 using AI methods. The final support schemes can be constructed by intelligent jumbos
 919 at the construction site. Once again, after the drilling and the measurement, the data on
 920 the new tunnel face are collected and a new round of the JIT design of the tunnel support
 921 is to be performed. Moreover, the employed techniques and aggregation algorithms in
 922 the proposed framework, such as the application of the IoT technique in the rock tunnel
 923 construction and performance of the algorithm on construction data, were individually
 924 validated in the reviewed studies. Hence, the reviewed studies can be considered as a
 925 validation of the proposed framework; thus, they reflect the rationality of the proposed
 926 framework.

927 Regarding the research gaps listed in Subsection 6.2, to accomplish the JIT design

928 of the tunnel support in **Fig.15** with an excellent performance, some possible
929 improvements are needed to remedy the listed limitations.

930 **(1) Adoption of the state-of-the-art deep learning technologies:** Our literature
931 review revealed that machine learning and deep learning technologies are particularly
932 successful in tasks associated with the image interpretation as they provide a high
933 accuracy and reasonable computational time [17,31,58,61,80]. Other studies have also
934 demonstrated the effectiveness of deep learning in the interpretation of point cloud data
935 [124]. Hence, regarding the challenge that the interpretation of data in some cases is
936 time-consuming, future researches can explore to use deep learning or other machine
937 learning approaches to accelerate the interpretation of point cloud data.

938 **(2) Automatic generation of numerical models:** An important factor affecting
939 the efficiency of numerical simulation is the model generation. Generally, the model is
940 generated manually using multiple pieces of information such as discontinuity
941 information [90,97], which is time-consuming and error-prone. The efficiency can be
942 greatly improved with the automatic generation of the model using certain structural
943 and surrounding rock mass information. In fact, Monsalve et al. [45] used the
944 interpreted information from TLS and generated a discrete fracture network for
945 discontinuous analysis, which indicated that the numerical model could be generated
946 automatically using on-site interpreted information. Further studies are needed to
947 investigate automatic integration of the geological, geotechnical, and hydrological
948 information into numerical models, and improvement of the effectiveness of methods.

949 **(3) Employment of parallel computing and cloud computing:** Parallel and
950 cloud computing are the computational methods aiming at improving computational
951 speed to solve complex computing problems. Wang et al. [19,125] used parallelization
952 and cloud computing to solve the problem of contact detection and computational
953 efficiency in 3D DDA, which is considered as one of the most powerful numerical
954 methods. Taking this as an example, further studies can integrate parallel and cloud
955 computing into the “acquisition-interpretation-aggregation” workflow, such as

956 continuous/discontinuous numerical analysis, to improve the computation speed.

957 **(4) Using ANN to directly get optimal support parameters:** ANN has been
958 proved to be an effective and powerful tool to model the nonlinear relationship between
959 support parameters and geological information [102,105]. Previous studies using ANN
960 relied on the information that exposed during the preliminary design stage. Hence, the
961 nonlinear relationship between the multi-source information exposed during
962 construction and support parameters can be explored, which can reduce labor cost and
963 improve construction efficiency.

964 **(5) Using ontology to represent knowledge:** The structured representation of
965 knowledge forms the basis of knowledge retrieval and reasoning. As an emerging
966 technology, ontology is widely used for knowledge sharing and reuse for its great
967 potential to address the problems related to holistic structural design [126]. Hence,
968 using ontology to represent tunnel design knowledge and design cases can be beneficial
969 for subsequent knowledge retrieval and reasoning. In addition, rule- and case-based
970 reasoning can be conducted to obtain the most appropriate support schemes based on
971 the structured knowledge.

972 **7 Conclusions**

973 This study presents a critical review on the design of the support during rock tunnel
974 construction from three perspectives: acquisition of on-site data, interpretation of raw
975 data and aggregation of interpreted data. The applications of IoT and IT in these three
976 perspectives have been thoroughly reviewed, including the time each technique costs,
977 its strengths and drawbacks, and its contribution to the design of the support. Based on
978 the review results, this study develops a conceptual framework for the JIT design of the
979 tunnel support, where research gaps, key concepts and possibilities of improvement
980 have been identified.

981 The overall challenges when performing the JIT design of the tunnel support have
982 been discussed. Time consumption, accuracy and degree of automation are three key
983 concepts in the JIT design of the tunnel support. Some appropriate and efficient

984 methods to realize the JIT design of the tunnel support have been highlighted and
985 recommended as follows: DP and TLS approaches for acquisition of tunnel face data,
986 GPR and TEM approaches for acquisition of data in front of the tunnel face, edge
987 detection, clustering and deep learning method for data interpretation, automatic model
988 generation for numerical analysis, and AI-supported techniques for data aggregation.

989 The adoption of the state-of-the-art AI technologies, such as ANN and deep
990 learning technologies, can significantly improve the efficiency of interpretation and
991 aggregation. Parallel computing and cloud computing are also promising areas that can
992 accelerate the computations involved in interpretation and aggregation. In addition, the
993 ontology technology can be employed in the design of the tunnel support to ease the
994 knowledge representation and reuse, thereby improving the performance of the support
995 design. The proposed framework for the JIT design of the tunnel support is a starting
996 point aiming to lead follow-up researches. The validation of the details in the proposed
997 framework shall be implemented correspondingly in future studies. In addition, the
998 feasibility of the proposed framework should be verified through practical applications
999 in engineering projects. Moreover, this review study contributes to elucidating the
1000 current state of the dynamic design of the tunnel support research and providing
1001 profound insights into the JIT design of the tunnel support research.

1002 **Declaration of Competing Interest**

1003 The authors declare that they have no known competing financial interests or
1004 personal relationships that could have appeared to influence the work reported in this
1005 paper.

1006 **Acknowledgement**

1007 This study was supported by the National Natural Science Foundation of China,
1008 High-Speed Railway Joint Fund (Grant No. U1934212).

1009 **References**

1010 [1] J. van Eldert, J. Funehag, D. Saiang, H. Schunnesson, Rock support
1011 prediction based on measurement while drilling technology, *Bulletin of*
1012 *Engineering Geology and the Environment*, 80 (2) (2021) 1449-1465.

-
- 1013 <http://dx.doi.org/10.1007/s10064-020-01957-x>
- 1014 [2] J. van Eldert, H. Schunnesson, D. Johansson, D. Saiang, Application
1015 of Measurement While Drilling Technology to Predict Rock Mass Quality and
1016 Rock Support for Tunnelling, *Rock Mechanics and Rock Engineering*, 53 (3)
1017 (2020) 1349-1358. <http://dx.doi.org/10.1007/s00603-019-01979-2>
- 1018 [3] Working Group Conventional Tunnelling ITA, General Report on
1019 Conventional Tunnelling Method, International Tunnelling and Underground
1020 Space Association, 2009, [https://tunnel.ita-
1021 aites.org/media/k2/attachments/public/ITA_Report_N2_WG19_P.pdf](https://tunnel.ita-aites.org/media/k2/attachments/public/ITA_Report_N2_WG19_P.pdf)
- 1022 [4] C. Haas, H.H. Einstein, Updating the decision aids for tunneling,
1023 *Journal of Construction Engineering and Management-ASCE*, 128 (1) (2002)
1024 40-48. [http://dx.doi.org/10.1061/\(asce\)0733-9364\(2002\)128:1\(40\)](http://dx.doi.org/10.1061/(asce)0733-9364(2002)128:1(40))
- 1025 [5] D.L. Boyd, G. Walton, W. Trainor-Guitton, Geostatistical estimation
1026 of Ground Class prior to and during excavation for the Caldecott Tunnel Fourth
1027 Bore project, *Tunnelling and Underground Space Technology*, 100 (2020).
1028 <http://dx.doi.org/10.1016/j.tust.2020.103391>
- 1029 [6] X.T. Feng, J.A. Hudson, *Rock engineering design*, CRC Press, 2011.
- 1030 [7] K. Sakai, T. Tani, T. Aoki, H. Ohtsu, Inclination monitoring at tunnel
1031 crown to predict change in ground stiffness ahead of excavation face,
1032 *Tunnelling and Underground Space Technology*, 104 (2020).
1033 <http://dx.doi.org/10.1016/j.tust.2020.103516>
- 1034 [8] B.W. Du, Y.L. Du, F. Xu, P. He, Conception and Exploration of Using
1035 Data as a Service in Tunnel Construction with the NATM, *Engineering*, 4 (1)
1036 (2018) 123-130. <http://dx.doi.org/10.1016/j.eng.2017.07.002>
- 1037 [9] X.T. Feng, C.Q. Zhang, S.L. Qiu, H. Zhou, Q. Jiang, S.J. Li, Dynamic
1038 design method for deep hard rock tunnels and its application, *Journal of Rock
1039 Mechanics and Geotechnical Engineering*, 8 (4) (2016) 443-461.
1040 <http://dx.doi.org/10.1016/j.jrmge.2016.01.004>
- 1041 [10] Specifications for Design of Highway Tunnels: JTG 3370.1-2018,
1042 Ministry of Transport of the People's Republic of China, Beijing, China, 2018.
- 1043 [11] Code for Design of Railway Tunnel: TB 10003-2016, China Railway
1044 Publishing House, Beijing, China, 2016.
- 1045 [12] J.M. Feng, C.W. Yan, L. Ye, X.Q. Ding, J.R. Zhang, Z.L. Li,
1046 Evaluation of installation timing of initial ground support for large-span tunnel
1047 in hard rock, *Tunnelling and Underground Space Technology*, 93 (2019).
1048 <http://dx.doi.org/10.1016/j.tust.2019.103087>
- 1049 [13] T.R. Reid, J.P. Harrison, A semi-automated methodology for
1050 discontinuity trace detection in digital images of rock mass exposures,
1051 *International Journal of Rock Mechanics and Mining Sciences*, 37 (7) (2000)
1052 1073-1089. [http://dx.doi.org/10.1016/s1365-1609\(00\)00041-1](http://dx.doi.org/10.1016/s1365-1609(00)00041-1)
- 1053 [14] S. Yang, S.M. Liu, N. Zhang, G.C. Li, J. Zhang, A fully automatic-
1054 image-based approach to quantifying the geological strength index of

1055 underground rock mass, International Journal of Rock Mechanics and Mining
1056 Sciences, 140 (2021). <http://dx.doi.org/10.1016/j.ijrmms.2020.104585>

1057 [15] B.V. Farahani, F. Barros, P.J. Sousa, P.P. Cacciari, P.J. Tavares, M.M.
1058 Futai, P. Moreira, A coupled 3D laser scanning and digital image correlation
1059 system for geometry acquisition and deformation monitoring of a railway tunnel,
1060 Tunnelling and Underground Space Technology, 91 (2019).
1061 <http://dx.doi.org/10.1016/j.tust.2019.102995>

1062 [16] S. Fekete, M. Diederichs, M. Lato, Geotechnical and operational
1063 applications for 3-dimensional laser scanning in drill and blast tunnels,
1064 Tunnelling and Underground Space Technology, 25 (5) (2010) 614-628.
1065 <http://dx.doi.org/10.1016/j.tust.2010.04.008>

1066 [17] J.Y. Chen, M.L. Zhou, H.W. Huang, D.M. Zhang, Z.C. Peng,
1067 Automated extraction and evaluation of fracture trace maps from rock tunnel
1068 face images via deep learning, International Journal of Rock Mechanics and
1069 Mining Sciences, 142 (2021). <http://dx.doi.org/10.1016/j.ijrmms.2021.104745>

1070 [18] A. Mitelmam, D. Elmo, Analysis of tunnel-support interaction using
1071 an equivalent boundary beam, Tunnelling and Underground Space Technology,
1072 84 (2019) 218-226. <http://dx.doi.org/10.1016/j.tust.2018.11.021>

1073 [19] X. Wang, W. Wu, H. Zhu, F. Liu, H. Zhang, J.-S. Lin, Three-
1074 dimensional discontinuous deformation analysis with explicit contact
1075 formulation and block-wise multicore CPU acceleration, Computers and
1076 Geotechnics, 139 (2021). <http://dx.doi.org/10.1016/j.compgeo.2021.104410>

1077 [20] J. Morgenroth, U.T. Khan, M.A. Perras, An Overview of
1078 Opportunities for Machine Learning Methods in Underground Rock
1079 Engineering Design, Geosciences, 9 (12) (2019).
1080 <http://dx.doi.org/10.3390/geosciences9120504>

1081 [21] E.F. Salmi, E.J. Sellers, A review of the methods to incorporate the
1082 geological and geotechnical characteristics of rock masses in blastability
1083 assessments for selective blast design, Engineering Geology, 281 (2021).
1084 <http://dx.doi.org/10.1016/j.enggeo.2020.105970>

1085 [22] R. Battulwar, M. Zare-Naghadehi, E. Emami, J. Sattarvand, A state-
1086 of-the-art review of automated extraction of rock mass discontinuity
1087 characteristics using three-dimensional surface models, Journal of Rock
1088 Mechanics and Geotechnical Engineering, 13 (4) (2021) 920-936.
1089 <http://dx.doi.org/10.1016/j.jrmge.2021.01.008>

1090 [23] S. Li, B. Liu, X. Xu, L. Nie, Z. Liu, J. Song, H. Sun, L. Chen, K. Fan,
1091 An overview of ahead geological prospecting in tunneling, Tunnelling and
1092 Underground Space Technology, 63 (2017) 69-94.
1093 <http://dx.doi.org/10.1016/j.tust.2016.12.011>

1094 [24] C.M. Chen, Searching for intellectual turning points: Progressive
1095 knowledge domain visualization, Proceedings of the National Academy of
1096 Sciences of the United States of America, 101 (2004) 5303-5310.

1097 <http://dx.doi.org/10.1073/pnas.0307513100>

1098 [25] L.V. Rabcewicz, The new Austrian tunnelling method, *Water Power*,

1099 (11) (1964) 453-457.

1100 [26] K.Y. Liu, B.G. Liu, Intelligent information-based construction in

1101 tunnel engineering based on the GA and CCGPR coupled algorithm, *Tunnelling*

1102 *and Underground Space Technology*, 88 (2019) 113-128.

1103 <http://dx.doi.org/10.1016/j.tust.2019.02.012>

1104 [27] F. Xu, S.c. Li, Q.q. Zhang, L.p. Li, S.s. Shi, Q. Zhang, A new type

1105 support structure introduction and its contrast study with traditional support

1106 structure used in tunnel construction, *Tunnelling and Underground Space*

1107 *Technology*, 63 (2017) 171-182. <http://dx.doi.org/10.1016/j.tust.2016.11.012>

1108 [28] J.Z. Huang, X.T. Feng, Y.Y. Zhou, C.X. Yang, Stability analysis of

1109 deep-buried hard rock underground laboratories based on

1110 stereophotogrammetry and discontinuity identification, *Bulletin of Engineering*

1111 *Geology and the Environment*, 78 (7) (2019) 5195-5217.

1112 <http://dx.doi.org/10.1007/s10064-019-01461-x>

1113 [29] F. Lemy, J. Hadjigeorgiou, Discontinuity trace map construction

1114 using photographs of rock exposures, *International Journal of Rock Mechanics*

1115 *and Mining Sciences*, 40 (6) (2003) 903-917. [http://dx.doi.org/10.1016/s1365-](http://dx.doi.org/10.1016/s1365-1609(03)00069-8)

1116 [1609\(03\)00069-8](http://dx.doi.org/10.1016/s1365-1609(03)00069-8)

1117 [30] G. Umili, S. Bonetto, A.M. Ferrero, An integrated multiscale

1118 approach for characterization of rock masses subjected to tunnel excavation,

1119 *Journal of Rock Mechanics and Geotechnical Engineering*, 10 (3) (2018) 513-

1120 522. <http://dx.doi.org/10.1016/j.jrmge.2018.01.007>

1121 [31] J. Chen, T. Yang, D. Zhang, H. Huang, Y. Tian, Deep learning based

1122 classification of rock structure of tunnel face, *Geoscience Frontiers*, 12 (1)

1123 (2021) 395-404. <http://dx.doi.org/10.1016/j.gsf.2020.04.003>

1124 [32] R. Garcia-Luna, S. Senent, R. Jurado-Pina, R. Jimenez, Structure

1125 from Motion photogrammetry to characterize underground rock masses:

1126 Experiences from two real tunnels, *Tunnelling and Underground Space*

1127 *Technology*, 83 (2019) 262-273. <http://dx.doi.org/10.1016/j.tust.2018.09.026>

1128 [33] Y. Wang, S.H. Wang, M.D. Guo, Z.H. Dong, Fast digital identification

1129 of joint information of tunnel work face and its stability analysis, *Chinese*

1130 *Journal of Geotechnical Engineering*, 33 (11) (2011) 1734-1739.

1131 <http://dx.doi.org/10.1097/RLU.0b013e3181f49ac7>

1132 [34] H. Zhu, W. Wu, J. Chen, G. Ma, X. Liu, X. Zhuang, Integration of

1133 three dimensional discontinuous deformation analysis (DDA) with binocular

1134 photogrammetry for stability analysis of tunnels in blocky rockmass, *Tunnelling*

1135 *and Underground Space Technology*, 51 (2016) 30-40.

1136 <http://dx.doi.org/10.1016/j.tust.2015.10.012>

1137 [35] J. Chen, H. Huang, M. Zhou, K. Chaiyasarn, Towards semi-automatic

1138 discontinuity characterization in rock tunnel faces using 3D point clouds,

1139 Engineering Geology, 291 (2021).
1140 <http://dx.doi.org/10.1016/j.enggeo.2021.106232>

1141 [36] Z. Xie, B.L. Chen, J.Y. Fu, Z.H. Zhu, J. Zheng, J.S. Yang, Digital
1142 identification and application of rock mass structure on tunnel excavation face
1143 based on computer vision 3D reconstruction, Journal of Railway Science and
1144 Engineering, 16 (04) (2019) 1001-1007. [http://dx.doi.org/10.19713/j.cnki.43-
1145 1423/u.2019.04.022](http://dx.doi.org/10.19713/j.cnki.43-1423/u.2019.04.022)

1146 [37] X. Li, Z. Chen, J. Chen, H. Zhu, Automatic characterization of rock
1147 mass discontinuities using 3D point clouds, Engineering Geology, 259 (2019).
1148 <http://dx.doi.org/10.1016/j.enggeo.2019.05.008>

1149 [38] B. Ghabraie, G. Ren, J. Smith, L. Holden, Application of 3D laser
1150 scanner, optical transducers and digital image processing techniques in physical
1151 modelling of mining-related strata movement, International Journal of Rock
1152 Mechanics and Mining Sciences, 80 (2015) 219-230.
1153 <http://dx.doi.org/10.1016/j.ijrmms.2015.09.025>

1154 [39] S. Chen, M.L. Walske, I.J. Davies, Rapid mapping and analysing rock
1155 mass discontinuities with 3D terrestrial laser scanning in the underground
1156 excavation, International Journal of Rock Mechanics and Mining Sciences, 110
1157 (2018) 28-35. <http://dx.doi.org/10.1016/j.ijrmms.2018.07.012>

1158 [40] C.Q. Li, H.L. Deng, C. Ge, S.M. Wang, G. Yang, S.L. Wu,
1159 Technology and application of 3D tunnel information monitoring, 6th
1160 International Conference on Electronics and Information Engineering (ICEIE),
1161 Vol. 9794, Dalian, PEOPLES R CHINA, 2015.
1162 <http://dx.doi.org/10.1117/12.2202347>

1163 [41] S. Fekete, M. Diederichs, Integration of three-dimensional laser
1164 scanning with discontinuum modelling for stability analysis of tunnels in blocky
1165 rockmasses, International Journal of Rock Mechanics and Mining Sciences, 57
1166 (2013) 11-23. <http://dx.doi.org/10.1016/j.ijrmms.2012.08.003>

1167 [42] R. Roncella, G. Forlani, F. Remondino, Photogrammetry for
1168 geological applications: automatic retrieval of discontinuity orientation in rock
1169 slopes, Conference Videometrics VIII, Vol. 5665, San Jose, CA, 2005, pp. 17-
1170 27. <http://dx.doi.org/10.1117/12.587822>

1171 [43] X. Li, J. Chen, H. Zhu, A new method for automated discontinuity
1172 trace mapping on rock mass 3D surface model, Computers & Geosciences, 89
1173 (2016) 118-131. <http://dx.doi.org/10.1016/j.cageo.2015.12.010>

1174 [44] P.P. Cacciari, M.M. Futai, Modeling a Shallow Rock Tunnel Using
1175 Terrestrial Laser Scanning and Discrete Fracture Networks, Rock Mechanics
1176 and Rock Engineering, 50 (5) (2017) 1217-1242.
1177 <http://dx.doi.org/10.1007/s00603-017-1166-6>

1178 [45] J.J. Monsalve, J. Baggett, R. Bishop, N. Ripepi, Application of laser
1179 scanning for rock mass characterization and discrete fracture network
1180 generation in an underground limestone mine, International Journal of Mining

-
- 1181 Science and Technology, 29 (1) (2019) 131-137.
1182 <http://dx.doi.org/10.1016/j.ijmst.2018.11.009>
- 1183 [46] S. Manzoor, S. Liaghat, A. Gustafson, D. Johansson, H. Schunnesson,
1184 Establishing relationships between structural data from close-range terrestrial
1185 digital photogrammetry and measurement while drilling data, Engineering
1186 Geology, 267 (2020). <http://dx.doi.org/10.1016/j.enggeo.2020.105480>
- 1187 [47] J. van Eldert, H. Schunnesson, D. Saiang, J. Funehag, Improved
1188 filtering and normalizing of Measurement-While-Drilling (MWD) data in
1189 tunnel excavation, Tunnelling and Underground Space Technology, 103 (2020).
1190 <http://dx.doi.org/10.1016/j.tust.2020.103467>
- 1191 [48] B.K. Mohammad, H. Robert, Processing of measurement while
1192 drilling data for rock mass characterization, International Journal of Mining
1193 Science and Technology, 26 (6) (2016) 989-994.
1194 <http://dx.doi.org/10.1016/j.ijmst.2016.09.005>
- 1195 [49] S. Manzoor, S. Liaghat, A. Gustafson, D. Johansson, H. Schunnesson,
1196 Rock mass characterization using MWD data and photogrammetry, Mining
1197 Goes Digital, CRC Press, 2019, ISBN 0429320779, pp. 217-225.
- 1198 [50] J. Navarro, J.A. Sanchidrian, P. Segarra, R. Castedo, E. Costamagna,
1199 L.M. Lopez, Detection of potential overbreak zones in tunnel blasting from
1200 MWD data, Tunnelling and Underground Space Technology, 82 (2018) 504-
1201 516. <http://dx.doi.org/10.1016/j.tust.2018.08.060>
- 1202 [51] K. Zhang, W. Wu, H. Zhu, L. Zhang, X. Li, H. Zhang, A modified
1203 method of discontinuity trace mapping using three-dimensional point clouds of
1204 rock mass surfaces, Journal of Rock Mechanics and Geotechnical Engineering,
1205 12 (3) (2020) 571-586. <http://dx.doi.org/10.1016/j.jrmge.2019.10.006>
- 1206 [52] S.-q. Sun, L.-p. Li, J. Wang, H. Liu, Z. Fang, X. Ba, Analysis and
1207 Prediction of Structural Plane Connectivity in Tunnel based on Digitalizing
1208 Image, Ksce Journal of Civil Engineering, 23 (6) (2019) 2679-2689.
1209 <http://dx.doi.org/10.1007/s12205-019-1000-7>
- 1210 [53] D. Deb, S. Hariharan, U.M. Rao, C.-H. Ryu, Automatic detection and
1211 analysis of discontinuity geometry of rock mass from digital images, Computers
1212 & Geosciences, 34 (2) (2008) 115-126.
1213 <http://dx.doi.org/10.1016/j.cageo.2007.03.007>
- 1214 [54] J. Chen, H. Zhu, X. Li, Automatic extraction of discontinuity
1215 orientation from rock mass surface 3D point cloud, Computers & Geosciences,
1216 95 (2016) 18-31. <http://dx.doi.org/10.1016/j.cageo.2016.06.015>
- 1217 [55] M. Azarafza, A. Ghazifard, H. Akgun, E. Asghari-Kaljahi,
1218 Development of a 2D and 3D computational algorithm for discontinuity
1219 structural geometry identification by artificial intelligence based on image
1220 processing techniques, Bulletin of Engineering Geology and the Environment,
1221 78 (5) (2019) 3371-3383. <http://dx.doi.org/10.1007/s10064-018-1298-2>
- 1222 [56] S.S. Leu, S.L. Chang, Digital image processing based approach for

1223 tunnel excavation faces, *Automation in Construction*, 14 (6) (2005) 750-765.
1224 <http://dx.doi.org/10.1016/j.autcon.2005.02.004>

1225 [57] J. Chen, X. Li, H. Zhu, Y. Rubin, Geostatistical method for inferring
1226 RMR ahead of tunnel face excavation using dynamically exposed geological
1227 information, *Engineering Geology*, 228 (2017) 214-223.
1228 <http://dx.doi.org/10.1016/j.enggeo.2017.08.004>

1229 [58] J. Chen, D. Zhang, H. Huang, M. Shadabfar, M. Zhou, T. Yang,
1230 Image-based segmentation and quantification of weak interlayers in rock tunnel
1231 face via deep learning, *Automation in Construction*, 120 (2020).
1232 <http://dx.doi.org/10.1016/j.autcon.2020.103371>

1233 [59] M.J. Lato, M.S. Diederichs, Mapping shotcrete thickness using
1234 LiDAR and photogrammetry data: Correcting for over-calculation due to
1235 rockmass convergence, *Tunnelling and Underground Space Technology*, 41
1236 (2014) 234-240. <http://dx.doi.org/10.1016/j.tust.2013.12.013>

1237 [60] M. Zhou, J. Chen, H. Huang, D. Zhang, S. Zhao, M. Shadabfar, Multi-
1238 source data driven method for assessing the rock mass quality of a NATM tunnel
1239 face via hybrid ensemble learning models, *International Journal of Rock
1240 Mechanics and Mining Sciences*, 147 (2021).
1241 <http://dx.doi.org/10.1016/j.ijrmms.2021.104914>

1242 [61] J. Chen, M. Zhou, D. Zhang, H. Huang, F. Zhang, Quantification of
1243 water inflow in rock tunnel faces via convolutional neural network approach,
1244 *Automation in Construction*, 123 (2021).
1245 <http://dx.doi.org/10.1016/j.autcon.2020.103526>

1246 [62] B. Leng, H. Yang, G. Hou, A. Lyamin, Rock mass trace line
1247 identification incorporated with grouping algorithm at tunnel faces, *Tunnelling
1248 and Underground Space Technology*, 110 (2021).
1249 <http://dx.doi.org/10.1016/j.tust.2021.103810>

1250 [63] S. Wang, P. Ni, M. Guo, Spatial characterization of joint planes and
1251 stability analysis of tunnel blocks, *Tunnelling and Underground Space
1252 Technology*, 38 (2013) 357-367. <http://dx.doi.org/10.1016/j.tust.2013.07.017>

1253 [64] S.Y. Qin, J.Y. Chen, D.M. Zhang, T.J. Yang, H.W. Huang, S. Zhao,
1254 Automatic Identification of Rock Structure at Tunnel Working Face Based on
1255 Deep Learning, *MODERN TUNNELLING TECHNOLOGY*, 58 (04) (2021)
1256 29-36. <http://dx.doi.org/10.13807/j.cnki.mtt.2021.04.004>

1257 [65] H.X. Liu, W.S. Li, H.Y. Zha, W.J. Jiang, T. Xu, Method for
1258 surrounding rock mass classification of highway tunnels based on deep learning
1259 technology, *Chinese Journal of Geotechnical Engineering*, 40 (10) (2018) 1809-
1260 1817. <http://dx.doi.org/10.11779/CJGE201810007>

1261 [66] S.C. Li, H.L. Liu, L.P. Li, S.S. Shi, Q.Q. Zhang, S.Q. Sun, J. Hu, A
1262 quantitative method for rock structure at working faces of tunnels based on
1263 digital images and its application, *Chinese Journal of Rock Mechanics and
1264 Engineering*, 36 (01) (2017) 1-9.

-
- 1265 <http://dx.doi.org/10.13722/j.cnki.jrme.2015.1751>
- 1266 [67] B. Leng, Y. Zhang, H. Yang, G.P. Hou, Rapid Recognition of Rock
1267 Mass Fractures in Tunnel Faces, Journal of Southwest Jiaotong University, 56
1268 (02) (2021) 246-252+322. [http://dx.doi.org/10.3969/j.issn.0258-
1269 2724.20190749](http://dx.doi.org/10.3969/j.issn.0258-2724.20190749)
- 1270 [68] H. Stille, A. Palmström, Classification as a tool in rock engineering,
1271 Tunnelling and Underground Space Technology, 18 (4) (2003) 331-345.
1272 [http://dx.doi.org/10.1016/S0886-7798\(02\)00106-2](http://dx.doi.org/10.1016/S0886-7798(02)00106-2)
- 1273 [69] M. Voge, M.J. Lato, M.S. Diederichs, Automated rockmass
1274 discontinuity mapping from 3-dimensional surface data, Engineering Geology,
1275 164 (2013) 155-162. <http://dx.doi.org/10.1016/j.enggeo.2013.07.008>
- 1276 [70] P.P. Cacciari, M.M. Futai, Mapping and characterization of rock
1277 discontinuities in a tunnel using 3D terrestrial laser scanning, Bulletin of
1278 Engineering Geology and the Environment, 75 (1) (2016) 223-237.
1279 <http://dx.doi.org/10.1007/s10064-015-0748-3>
- 1280 [71] D. Xu, X.T. Feng, S.J. Li, S.Y. Wu, S.L. Qiu, Y.Y. Zhou, Y.H. Gao,
1281 In-situ testing technique for tunnel deformation and structural plane of rock
1282 mass based on contactless laser scanning method and its application, Chinese
1283 Journal of Geotechnical Engineering, 40 (07) (2018) 1336-1343.
1284 <http://dx.doi.org/10.11779/CJGE201807022>
- 1285 [72] G. Walton, M.S. Diederichs, K. Weinhardt, D. Delaloye, M.J. Lato, A.
1286 Punkkinen, Change detection in drill and blast tunnels from point cloud data,
1287 International Journal of Rock Mechanics and Mining Sciences, 105 (2018) 172-
1288 181. <http://dx.doi.org/10.1016/j.ijrmms.2018.03.004>
- 1289 [73] Y. Kim, A. Bruland, Analysis and Evaluation of Tunnel Contour
1290 Quality Index, Automation in Construction, 99 (2019) 223-237.
1291 <http://dx.doi.org/10.1016/j.autcon.2018.12.008>
- 1292 [74] M. Galende-Hernandez, M. Menendez, M.J. Fuente, G.I. Sainz-
1293 Palmero, Monitor-While-Drilling-based estimation of rock mass rating with
1294 computational intelligence: The case of tunnel excavation front, Automation in
1295 Construction, 93 (2018) 325-338.
1296 <http://dx.doi.org/10.1016/j.autcon.2018.05.019>
- 1297 [75] J. van Eldert, J. Funehag, H. Schunnesson, D. Saiang, Drill
1298 Monitoring for Rock Mass Grouting: Case Study at the Stockholm Bypass,
1299 Rock Mechanics and Rock Engineering, 54 (2) (2021) 501-511.
1300 <http://dx.doi.org/10.1007/s00603-020-02279-w>
- 1301 [76] L. Bu, S. Li, S. Shi, L. Li, Y. Zhao, Z. Zhou, L. Nie, H. Sun,
1302 Application of the comprehensive forecast system for water-bearing structures
1303 in a karst tunnel: a case study, Bulletin of Engineering Geology and the
1304 Environment, 78 (1) (2019) 357-373. [http://dx.doi.org/10.1007/s10064-017-
1305 1114-4](http://dx.doi.org/10.1007/s10064-017-1114-4)
- 1306 [77] F. Sengani, The use of ground Penetrating Radar to distinguish

1307 between seismic and non-seismic hazards in hard rock mining, *Tunnelling and*
1308 *Underground Space Technology*, 103 (2020).
1309 <http://dx.doi.org/10.1016/j.tust.2020.103470>

1310 [78] M. Liu, Z. Liu, D. Zhou, R. Lan, H. Wu, Recognition method of
1311 typical anomalies during karst tunnel construction using GPR attributes and
1312 Gaussian processes, *Arabian Journal of Geosciences*, 13 (16) (2020).
1313 <http://dx.doi.org/10.1007/s12517-020-05782-0>

1314 [79] T.H. Ling, S. Zhang, S.R. Li, Hibert-Huang Transform Method For
1315 Detection Signal Of Tunnel Geological Prediction Using Ground Penetrating
1316 Radar, *Chinese Journal of Rock Mechanics and Engineering*, 31 (07) (2012)
1317 1422-1428. <http://dx.doi.org/10.3969/j.issn.1000-6915.2012.07.015>

1318 [80] H. Qin, D. Zhang, Y. Tang, Y. Wang, Automatic recognition of tunnel
1319 lining elements from GPR images using deep convolutional networks with data
1320 augmentation, *Automation in Construction*, 130 (2021).
1321 <http://dx.doi.org/10.1016/j.autcon.2021.103830>

1322 [81] L. Bu, S.C. Li, S.S. Shi, X.K. Xie, L.P. Li, Z.Q. Zhou, Z.J. Wen, A
1323 New Advance Classification Method for Surrounding Rock in Tunnels Based
1324 on the Set-Pair Analysis and Tunnel Seismic Prediction System, *Geotechnical*
1325 *and Geological Engineering*, 36 (4) (2018) 2403-2413.
1326 <http://dx.doi.org/10.1007/s10706-018-0471-5>

1327 [82] S.S. Shi, S.C. Li, L.P. Li, Z.Q. Zhou, J. Wang, Advance optimized
1328 classification and application of surrounding rock based on fuzzy analytic
1329 hierarchy process and Tunnel Seismic Prediction, *Automation in Construction*,
1330 37 (2014) 217-222. <http://dx.doi.org/10.1016/j.autcon.2013.08.019>

1331 [83] H.-K. Tzou, T.-S. Chu, T.-Y. Liu, Enhancing the safety management
1332 of NATM using the tunnel seismic prediction method: a case study, *Innovative*
1333 *Infrastructure Solutions*, 5 (3) (2020). [http://dx.doi.org/10.1007/s41062-020-](http://dx.doi.org/10.1007/s41062-020-00357-0)
1334 [00357-0](http://dx.doi.org/10.1007/s41062-020-00357-0)

1335 [84] A. Alimoradi, A. Moradzadeh, R. Naderi, M.Z. Salehi, A. Etemadi,
1336 Prediction of geological hazardous zones in front of a tunnel face using TSP-
1337 203 and artificial neural networks, *Tunnelling and Underground Space*
1338 *Technology*, 23 (6) (2008) 711-717.
1339 <http://dx.doi.org/10.1016/j.tust.2008.01.001>

1340 [85] A. Esmailzadeh, R. Mikaeil, E. Shafei, G. Sadegheslam, Prediction of
1341 rock mass rating using TSP method and statistical analysis in Semnan Rooziyeh
1342 spring conveyance tunnel, *Tunnelling and Underground Space Technology*, 79
1343 (2018) 224-230. <http://dx.doi.org/10.1016/j.tust.2018.05.001>

1344 [86] H. Fan, L. Li, H. Liu, S. Shi, J. Hu, S. Zhou, Advanced Stability
1345 Analysis of the Tunnels in Jointed Rock Mass Based on TSP and DEM, *Ksce*
1346 *Journal of Civil Engineering*, 25 (4) (2021) 1491-1503.
1347 <http://dx.doi.org/10.1007/s12205-021-0170-2>

1348 [87] C. Cao, C. Shi, M. Lei, W. Yang, J. Liu, Squeezing failure of tunnels:

1349 A case study, *Tunnelling and Underground Space Technology*, 77 (2018) 188-
1350 203. <http://dx.doi.org/10.1016/j.tust.2018.04.007>

1351 [88] L. Nie, Y. Zhang, M. Su, Y. Geng, Z. Liu, K. Fan, B. Yan, J. Shen,
1352 Comprehensive Ahead Prospecting of Tunnels in Severely Weathered Rock
1353 Mass Environments with High Water Inrush Risk: A Case Study in Shaanxi
1354 Province, *Advances in Civil Engineering*, 2020 (2020).
1355 <http://dx.doi.org/10.1155/2020/8867382>

1356 [89] A.T.C. Goh, W. Zhang, Y. Zhang, Y. Xiao, Y. Xiang, Determination
1357 of earth pressure balance tunnel-related maximum surface settlement: a
1358 multivariate adaptive regression splines approach, *Bulletin of Engineering
1359 Geology and the Environment*, 77 (2) (2018) 489-500.
1360 <http://dx.doi.org/10.1007/s10064-016-0937-8>

1361 [90] A. Kaya, A. Sayin, Engineering geological appraisal and preliminary
1362 support design for the Salarha Tunnel, Northeast Turkey, *Bulletin of
1363 Engineering Geology and the Environment*, 78 (2) (2019) 1095-1112.
1364 <http://dx.doi.org/10.1007/s10064-017-1177-2>

1365 [91] E. Sopacı, H. Akgün, Engineering geological investigations and the
1366 preliminary support design for the proposed Ordu Peripheral Highway Tunnel,
1367 Ordu, Turkey, *Engineering Geology*, 96 (1-2) (2008) 43-61.
1368 <http://dx.doi.org/10.1016/j.enggeo.2007.09.005>

1369 [92] M. Kanik, Z. Gurocak, S. Alemdag, A comparison of support systems
1370 obtained from the RMR89 and RMR14 by numerical analyses: Macka Tunnel
1371 project, NE Turkey, *Journal of African Earth Sciences*, 109 (2015) 224-238.
1372 <http://dx.doi.org/10.1016/j.jafrearsci.2015.05.025>

1373 [93] E.B. Aygar, C. Gokceoglu, A special support design for a large-span
1374 tunnel crossing an active fault (T9 Tunnel, Ankara-Sivas High-Speed Railway
1375 Project, Turkey), *Environmental Earth Sciences*, 80 (1) (2021).
1376 <http://dx.doi.org/10.1007/s12665-020-09328-1>

1377 [94] L.Y. Zhang, H.H. Zhu, Three-dimensional Hoek-Brown strength
1378 criterion for rocks, *Journal of Geotechnical and Geoenvironmental Engineering*,
1379 133 (9) (2007) 1128-1135. [http://dx.doi.org/10.1061/\(asce\)1090-
1380 0241\(2007\)133:9\(1128\)](http://dx.doi.org/10.1061/(asce)1090-0241(2007)133:9(1128))

1381 [95] C. Xu, C.C. Xia, S.G. Du, Simplified solution for viscoelastic-plastic
1382 interaction between tunnel support and surrounding rock based on MC and GZZ
1383 strength criteria, *Computers and Geotechnics*, 139 (2021).
1384 <http://dx.doi.org/10.1016/j.compgeo.2021.104393>

1385 [96] Y. Xing, P.H.S.W. Kulatilake, L.A. Sandbak, Investigation of Rock
1386 Mass Stability Around the Tunnels in an Underground Mine in USA Using
1387 Three-Dimensional Numerical Modeling, *Rock Mechanics and Rock
1388 Engineering*, 51 (2) (2018) 579-597. [http://dx.doi.org/10.1007/s00603-017-
1389 1336-6](http://dx.doi.org/10.1007/s00603-017-1336-6)

1390 [97] F.Y. Hsiao, C.L. Wang, J.C. Chern, Numerical simulation of rock

1391 deformation for support design in tunnel intersection area, *Tunnelling and*
1392 *Underground Space Technology*, 24 (1) (2009) 14-21.
1393 <http://dx.doi.org/10.1016/j.tust.2008.01.003>

1394 [98] C. Sun, D.X. Chen, L.G. Wang, L. Wu, Quantitative evaluation of the
1395 constraint effect and stability of tunnel lining support, *Tunnelling and*
1396 *Underground Space Technology*, 112 (2021).
1397 <http://dx.doi.org/10.1016/j.tust.2021.103920>

1398 [99] M.R. Zareifard, An analytical solution for design of pressure tunnels
1399 considering seepage loads, *Applied Mathematical Modelling*, 62 (2018) 62-85.
1400 <http://dx.doi.org/10.1016/j.apm.2018.05.032>

1401 [100] Y. Su, Y. Su, M. Zhao, N. Vlachopoulos, Tunnel Stability
1402 Analysis in Weak Rocks Using the Convergence Confinement Method, *Rock*
1403 *Mechanics and Rock Engineering*, 54 (2) (2021) 559-582.
1404 <http://dx.doi.org/10.1007/s00603-020-02304-y>

1405 [101] S.C. Jong, D.E.L. Ong, E. Oh, State-of-the-art review of
1406 geotechnical-driven artificial intelligence techniques in underground soil-
1407 structure interaction, *Tunnelling and Underground Space Technology*, 113
1408 (2021). <http://dx.doi.org/10.1016/j.tust.2021.103946>

1409 [102] Y.X. Xia, J.L. Qiu, Y.D. Wang, Application of artificial neural
1410 network in highway tunnel's support design, *Journal of Chang'an University*
1411 (Natural Science Edition), (02) (2005) 69-72.
1412 <http://dx.doi.org/10.19721/j.cnki.1671-8879.2005.02.016>

1413 [103] J. Liu, Y. Jiang, S. Ishizu, O. Sakaguchi, Estimation of tunnel
1414 support pattern selection using artificial neural network, *Arabian Journal of*
1415 *Geosciences*, 13 (9) (2020). <http://dx.doi.org/10.1007/s12517-020-05311-z>

1416 [104] J. Liu, Y. Jiang, W. Han, O. Sakaguchi, Optimized ANN model
1417 for predicting rock mass quality ahead of tunnel face using measure-while-
1418 drilling data, *Bulletin of Engineering Geology and the Environment*, 80 (3)
1419 (2021) 2283-2305. <http://dx.doi.org/10.1007/s10064-020-02057-6>

1420 [105] W. Nie, Z.Y. Zhao, A.T.C. Goh, M.K. Song, W. Guo, X. Zhu,
1421 Performance based support design for horseshoe-shaped rock caverns using 2D
1422 numerical analysis, *Engineering Geology*, 245 (2018) 266-279.
1423 <http://dx.doi.org/10.1016/j.enggeo.2018.09.007>

1424 [106] M.I. Alvarez-Fernandez, M.B. Prendes-Gero, J.M. Drouet, F.
1425 Lopez-Gayarre, J. Rodriguez-Vigil Junco, Application of genetic algorithms in
1426 the optimisation of steel rib supports, *Tunnelling and Underground Space*
1427 *Technology*, 103 (2020). <http://dx.doi.org/10.1016/j.tust.2020.103462>

1428 [107] R. Gholami, V. Rasouli, A. Alimoradi, Improved RMR Rock
1429 Mass Classification Using Artificial Intelligence Algorithms, *Rock Mechanics*
1430 *and Rock Engineering*, 46 (5) (2013) 1199-1209.
1431 <http://dx.doi.org/10.1007/s00603-012-0338-7>

1432 [108] K. Liu, B. Liu, Y. Fang, An intelligent model based on statistical

1433 learning theory for engineering rock mass classification, Bulletin of
1434 Engineering Geology and the Environment, 78 (6) (2019) 4533-4548.
1435 <http://dx.doi.org/10.1007/s10064-018-1419-y>

1436 [109] F. Li, A. Jiang, S. Zheng, Anchoring Parameters Optimization of
1437 Tunnel Surrounding Rock Based on Particle Swarm Optimization, Geotechnical
1438 and Geological Engineering, 39 (6) (2021) 4533-4543.
1439 <http://dx.doi.org/10.1007/s10706-021-01782-3>

1440 [110] A.N. Jiang, S.Y. Wang, S.L. Tang, Feedback analysis of tunnel
1441 construction using a hybrid arithmetic based on Support Vector Machine and
1442 Particle Swarm Optimisation, Automation in Construction, 20 (4) (2011) 482-
1443 489. <http://dx.doi.org/10.1016/j.autcon.2010.11.016>

1444 [111] Y. Yun, G. Kaneko, H. Kusumi, A. Nishio, T. Kurotani, Design
1445 for Support Patterns of NATM Tunnel Using Machine Learning, 3rd
1446 International Conference on Information Technology in Geo-Engineering
1447 (ICITG), Guimaraes, PORTUGAL, 2019, pp. 376-382.
1448 http://dx.doi.org/10.1007/978-3-030-32029-4_32

1449 [112] M. Wang, S. Zhao, J. Tong, Z. Wang, M. Yao, J. Li, W. Yi,
1450 Intelligent classification model of surrounding rock of tunnel using drilling and
1451 blasting method, Underground Space, 6 (5) (2021) 539-550.
1452 <http://dx.doi.org/10.1016/j.undsp.2020.10.001>

1453 [113] Y. An, H. Li, T. Su, Y. Wang, Determining Uncertainties in AI
1454 Applications in AEC Sector and their Corresponding Mitigation Strategies,
1455 Automation in Construction, 131 (2021).
1456 <http://dx.doi.org/10.1016/j.autcon.2021.103883>

1457 [114] S. Madhu, C.H. Juang, J.W. Chen, D.H. Lee, A knowledge based
1458 approach to rock mass classification and tunnel support selection, Civil
1459 Engineering Systems, 12 (4) (1995) 307-325.
1460 <http://dx.doi.org/10.1080/02630259508970179>

1461 [115] K.Y. Liu, C.S. Qiao, S.F. Tian, Design of tunnel shotcrete-bolting
1462 support based on a support vector machine approach, International Journal of
1463 Rock Mechanics and Mining Sciences, 41 (3) (2004) 510-511.
1464 <http://dx.doi.org/10.1016/j.ijrmms.2003.12.041>

1465 [116] S. Sebbeh-Newton, S. Ismail, H. Zabidi, Prediction of Rock Mass
1466 Rating using Adaptive Neuro-Fuzzy Inference System (ANFIS) for NATM-3 of
1467 Pahang-Selangor Raw Water Transfer Tunnel (PSRWT) Project, Malaysia,
1468 3rd International Postgraduate Conference on Materials, Minerals and Polymer
1469 (MAMIP), Vol. 2267, Penang, MALAYSIA, 2019.
1470 <http://dx.doi.org/10.1063/5.0016415>

1471 [117] Z. Wang, Research on Intelligent Construction Technology for
1472 High-speed Railway Mountain Tunnel: a Case Study of Hubei Section of
1473 Zhengzhou-Wanzhou High-speed Railway, Journal of the China railway society,
1474 42 (02) (2020) 86-95. <http://dx.doi.org/10.3969/j.issn.1001-8360.2020.02.012>

1475 [118] C.S. Qiao, L.P. Wei, Intelligent methods and its integration for
1476 bolt-shotcrete support design of underground rock excavation, Chinese Journal
1477 of Rock Mechanics and Engineering, (05) (2004) 781-785.
1478 <http://dx.doi.org/10.3321/j.issn:1000-6915.2004.05.014>

1479 [119] S.H. Wang, F.S. Zhu, K. Zhang, B. Liu, Intelligent decision-
1480 making aided system for rock tunnel construction, Chinese Journal of Rock
1481 Mechanics and Engineering, (04) (2002) 590-594.
1482 <http://dx.doi.org/10.3321/j.issn:1000-6915.2002.04.029>

1483 [120] J.H. Garrett, Where and why artificial neural networks are
1484 applicable in civil engineering, Journal of Computing in Civil Engineering, 8 (2)
1485 (1994) 129-130. [http://dx.doi.org/10.1061/\(asce\)0887-3801\(1994\)8:2\(129\)](http://dx.doi.org/10.1061/(asce)0887-3801(1994)8:2(129))

1486 [121] Y. Sugimori, K. Kusunoki, F. Cho, S. Uchikawa, Toyota
1487 Production System And Kanban System Materialization Of Just-in-time And
1488 Respect-for-human System, International Journal of Production Research, 15 (6)
1489 (1977) 553-564. <http://dx.doi.org/10.1080/00207547708943149>

1490 [122] T. Sukanuma, T. Ogasawara, M. Takeuchi, T. Yasue, M.
1491 Kawahito, K. Ishizaki, H. Komatsu, T. Nakatani, Overview of the IBM Java
1492 just-in-time compiler, Ibm Systems Journal, 39 (1) (2000) 175-193.
1493 <http://dx.doi.org/10.1147/sj.391.0175>

1494 [123] M. Rasouli, Engineering geological studies of the diversion
1495 tunnel, focusing on stabilization analysis and support design, Iran, Engineering
1496 Geology, 108 (3-4) (2009) 208-224.
1497 <http://dx.doi.org/10.1016/j.enggeo.2009.07.007>

1498 [124] H.W. Huang, W. Cheng, M.L. Zhou, J.Y. Chen, S. Zhao, Towards
1499 Automated 3D Inspection of Water Leakages in Shield Tunnel Linings Using
1500 Mobile Laser Scanning Data, Sensors, 20 (22) (2020).
1501 <http://dx.doi.org/10.3390/s20226669>

1502 [125] X. Wang, H. Li, W. Wu, H. Zhu, F. Liu, H. Zhang, Research
1503 progress of contact detection and cloud computing for 3D parallel explicit
1504 discontinuous deformation analysis, Hazard Control in Tunnelling and
1505 Underground Engineering, 3 (03) (2021) 111-118.
1506 <http://dx.doi.org/10.19952/j.cnki.2096-5052.2021.03.12>

1507 [126] G. Ren, R. Ding, H. Li, Building an ontological knowledgebase
1508 for bridge maintenance, Advances in Engineering Software, 130 (2019) 24-40.
1509 <http://dx.doi.org/10.1016/j.advengsoft.2019.02.001>

1510

Declaration of interests

The authors declare that they have no known competing financial interests or personal relationships that could have appeared to influence the work reported in this paper.

The authors declare the following financial interests/personal relationships which may be considered as potential competing interests: